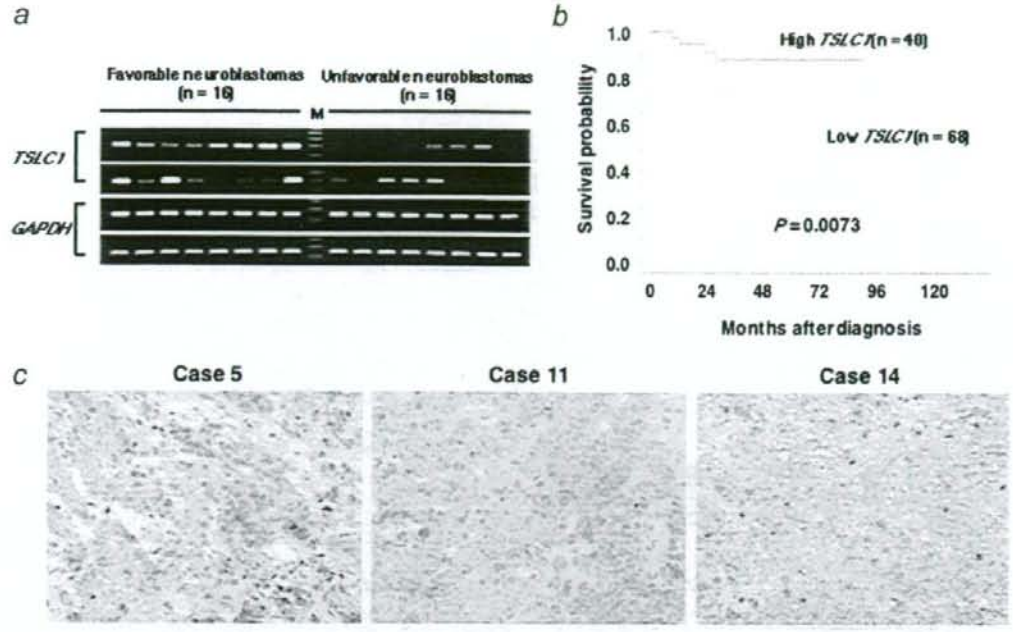

FIGURE 2 – Expression levels of *TSLC1* in primary neuroblastomas. (*a*) Expression of *TSLC1* in 16 favorable neuroblastomas bearing single copy of *MYCN* (Stage 1, higher expression levels of *TrkA*) and 16 unfavorable ones carrying *MYCN* amplification (stages 3 and 4, lower expression levels of *TrkA*). Total RNA was prepared from the indicated neuroblastoma tissues, reverse transcribed and amplified by PCR to examine the expression levels of *TSLC1*. *GAPDH* serves as an internal control. (*b*) Kaplan-Meier survival curves of patients with neuroblastomas based on higher or lower expression levels of *TSLC1*. Expression levels of *TSLC1* in 108 primary neuroblastoma samples categorized by their clinical stage were examined by a quantitative real-time PCR. Relative expression levels of *TSLC1* mRNA were determined by calculating the ratio between *GAPDH* and *TSLC1*. (*c*) Immunohistochemical analysis. Tumor samples derived from Case 5 (favorable neuroblastoma bearing single copy of *MYCN*), Case 11 (unfavorable neuroblastoma with *MYCN* amplification) and Case 14 (unfavorable neuroblastoma carrying single copy of *MYCN*) were fixed and stained with polyclonal anti-TSLC1 antibody.

primary neuroblastoma but not in neuroblastoma-derived cell lines.

Lower expression levels of TSLC1 are associated with poor outcome of neuroblastoma

To evaluate whether there could exist a possible relationship between *TSLC1* expression levels and clinicopathological factors of neuroblastoma patients, we have performed a quantitative real-time PCR. For this purpose, total RNA prepared from 108 primary neuroblastoma samples was subjected to a quantitative real-time PCR. According to the mean values of its expression levels obtained from a quantitative real-time PCR, these patients were divided into 2 groups including 40 patients with tumors expressing higher levels of *TSLC1* (High *TSLC1*) and 68 patients with tumors expressing lower levels of *TSLC1* (Low *TSLC1*). As shown in Table I, the significant differences were detectable between the above-mentioned 2 groups with respect to INSS stage, Shimada's pathological classification, copy number of *MYCN*, *TrkA* expression levels and DNA index. In contrast, no significant differences were observed between them with respect to their age, tumor origin and LOH on *TSLC1* locus.

We then examined whether there could exist a possible correlation between the expression levels of *TSLC1* in primary neuroblastomas and the survival of patients with neuroblastomas. The log-rank test showed that lower expression levels of *TSLC1* significantly correlate with unfavorable outcome ($p = 0.007$) as shown

TABLE I – CORRELATION BETWEEN *TSLC1* EXPRESSION AND OTHER PROGNOSTIC FACTORS OF NEUROBLASTOMA

Terms	*TSLC1* expression		*p*-Value
	High *TSLC1* ($n = 40$)	Low *TSLC1* ($n = 68$)	
Age (year)			
<1.5	23	29	
>1.5	17	39	0.1646
Tumor origin			
Adrenal grand	20	36	
Others	20	30	0.6915
Stage			
1, 2, 4S	24	25	
3, 4	16	43	0.0274
Shimada pathology			
Favorable	31	35	
Unfavorable	6	22	0.0227
MYCN copy number			
Single	38	51	
Amplified	2	17	0.0086
TrkA expression			
High	28	28	
Low	12	37	0.0090
DNA index			
Diploidy	8	39	
Aneuploidy	28	19	<0.0001
LOH			
(−)	18	29	
(+)	9	16	>0.9999

TABLE II – IMMUNOHISTOCHEMICAL ANALYSIS OF *TSLC1* EXPRESSION IN PRIMARY NEUROBLASTOMAS

Case	Age/Gender	*MYCN*	INPC	Primary site	Stage (INSS)	TSLC1
4	6 m/M	NA	NBL, Poorly diff., Low MKI, FH	Mediastinum	Stage 1	(+)
5	7 m/M	NA	NBL, Poorly diff., Low MKI, FH	Adrenal	Stage 1	(+)
6	9 m/M	NA	NBL, Poorly diff., Low MKI, FH	Adrenal	Stage 1	(+)
7	25 m/M	NA	NBL, Differentiating, Low MKI, FH	Adrenal	Stage 4	(+)
8	29 m/M	NA	NBL, Differentiating, Low MKI, FH	Mediastinum	Stage 2	(+)
9	13 m/M	A	NBL, Poorly diff., High MKI, UH	Adrenal	Stage 4	(−)
10	13 m/M	A	NBL, Poorly diff., Low MKI, UH	Abdominal	Stage 4	(−)
11	18 m/M	A	NBL, Poorly diff., Low MKI, UH	Adrenal	Stage 3	(−)
12	8 y/M	NA	NBL, Poorly diff., Low MKI, UH	Adrenal	Stage 4	(+)
13	8 m/M	NA	nGNB (NBL, poorly diff., Low MKI), UH	Mediastinum	Stage 2	(−)/(+)[1]
14	20 m/M	NA	NBL, Poorly diff., Low MKI, UH	Adrenal	Stage 3	(+)

m, months; y, years; M, male; NA, not amplified; A, amplified; NBL, neuroblastoma; nGNB, nodular ganglioneuroblastoma; MKI, mitosis-karyorrhexis index; FH, favorable histology; UH, unfavorable histology; (+), positive; (−), negative.
[1]Neuroblastoma component showed negative of TSLC1 signals, whereas ganglioneuroma showed positive of TSLC1 signals.

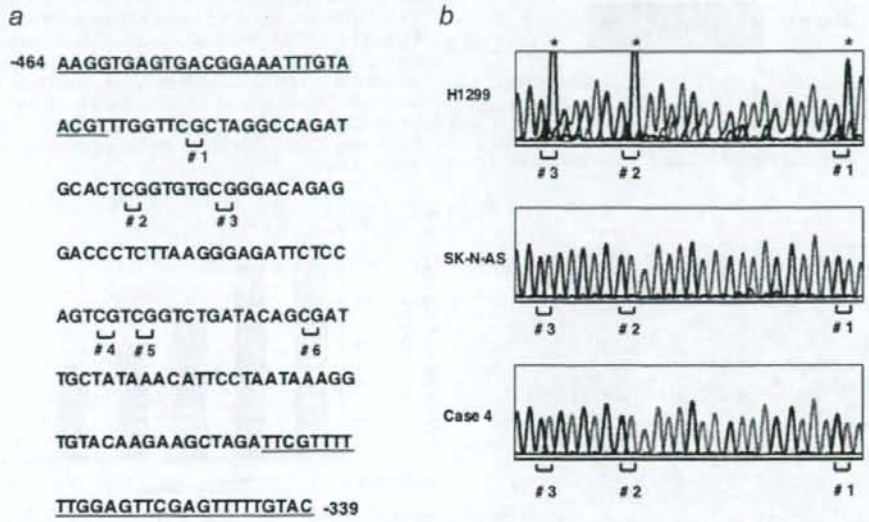

FIGURE 3 – Bisulfite-sequencing analysis of *TSLC1* gene promoter in neuroblastoma-derived cell lines and primary neuroblastomas. (*a*) Nucleotide sequence spanning from −464 to −339 relative to the translational initiation site (+1). Six CpG sites are shown. Primer sequences used for PCR-based amplification are underlined. (*b*) Bisulfite-sequencing analysis. Sequencing histograms showing the methylation status of CpG sites (#1, #2 and #3) are depicted. Asterisks indicate the positions of the methylated cytosine residues at the indicated CpG sites. H1299 cells were used as a positive control. [Color figure can be viewed in the online issue, which is available at www.interscience.wiley.com.]

in Kaplan-Meier cumulative survival curves (Fig. 2*b* and Supplementary Table I). Additionally, multivariable Cox analysis demonstrated that only clinical stage and *MYCN* amplification are significantly associated with their survival (Supplementary Table II), suggesting that *TSLC1* expression levels strongly correlate with these factors.

To further confirm the expression levels of TSLC1 in primary neuroblastomas, we employed immunohistochemical staining of TSLC1 in 11 primary neuroblastomas, including 5 favorable neuroblastomas bearing single copy of *MYCN*, 3 unfavorable neuroblastomas carrying single copy of *MYCN* and 3 unfavorable neuroblastomas with *MYCN* amplification. As shown in Figure 2*c*, TSLC1 appeared to be detectable at the cell–cell boundary of the tumors (cases 5 and 14) but not in Case 11. The immunohistochemical data were summarized in Table II. TSLC1 was detectable in tumors with favorable histology bearing single copy of *MYCN* (cases 4–8), whereas cases 9–11 with unfavorable histology carrying *MYCN* amplification did not express TSLC1. In addition, Case 13 was a nodular ganglioneuroblastoma whose ganglioneuroma and neuroblastoma components were TSLC1-positive and -negative, respectively. Of note, TSLC1 was detected in tumors with unfavorable histology bearing single copy of *MYCN* (cases 12–14). These observations indicate that there exists an inverse relationship between the expression levels of TSLC1 and *MYCN* amplification in primary neuroblastomas.

No promoter methylation of TSLC1 gene in neuroblastoma cell lines and primary neuroblastomas

Based on our present results, lower expression levels of *TSLC1* gene in unfavorable neuroblastomas might not be due to allelic loss of *TSLC1* locus. Since accumulating evidence strongly suggests that the downregulation of *TSLC1* in several cancers is associated with the hypermethylation of its promoter region,[9,11,12,24,26–29] we sought to examine whether the hypermethylation of *TSLC1* promoter region could be detectable in unfavorable neuroblastomas. For this purpose, we directly examined the methylation status of 6 cytosine residues of CpG sites within a putative *TSLC1* promoter region (Fig. 3*a*) by bisulfite-sequencing in 27 cell lines and 115 primary neuroblastomas. Sodium bisulfite modification of genomic DNA converts unmethylated cytosine residues to uracil residues but does not affect methylated cytosine residues. Unexpectedly, methylated cytosines

were undetectable in all primary neuroblastomas and cell lines, whereas hypermethylation was readily detected in human lung adenocarcinoma-derived H1299 cell line used as a positive control (Fig. 3*b*). Our present findings ruled out the possibility that the hypermethylation of *TSLC1* promoter region contributes to the downregulation of *TSLC1* gene in unfavorable neuroblastomas. Of note, the treatment of neuroblastoma-derived SH-SY5Y and CHP-134 cells with TSA (trichostatin A) resulted in a remarkable upregulation of *TSLC1* (Fig. 4). Since TSA is a histone deacetylase inhibitor, it is possible that the acetylation status of histone plays an important role in the regulation of *TSLC1* expression.

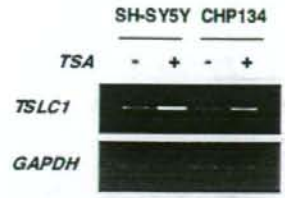

FIGURE 4 – Upregulation of *TSLC1* in cells exposed to TSA. SH-SY5Y and CHP-134 cells were treated with TSA (at a final concentration of 100 ng/ml) or left untreated. Twelve hours after treatment, total RNA was prepared and analyzed for the expression levels of *TSLC1* by semiquantitative RT-PCR. *GAPDH* was used as an internal control.

TSLC1 has an ability to suppress cell growth of neuroblastoma cells

To examine whether TSLC1 could have an ability to suppress neuroblastoma cell proliferation, we performed colony formation assays. Neuroblastoma-derived SH-SY5Y cells were transfected with or without the increasing amounts of the TSLC1 expression plasmid and maintained in fresh medium containing hygromycin for 14 days. As shown in Figure 5*a*, number of drug-resistant colonies was significantly reduced in a dose-dependent manner as compared with that in cells transfected with the empty plasmid alone. Similar results were also obtained in neuroblastoma-derived SK-N-AS cells (Supplementary Fig. 2). Next, we sought to examine a possible effect of the endogenous TSLC1 on neuroblastoma cell growth. To this end, SH-SY5Y cells were transiently transfected with control siRNA or siRNA against TSLC1. As shown in Figure 5*b*, siRNA-mediated silencing of the endogenous *TSLC1* was successful under our experimental conditions. Consistent with the present results obtained from colony formation assays, siRNA-mediated knockdown of TSLC1 resulted in an accelerated cell proliferation relative to the control cells ($p < 0.05$). Thus, it is likely that TSLC1 has an ability to suppress neuroblastoma cell proliferation.

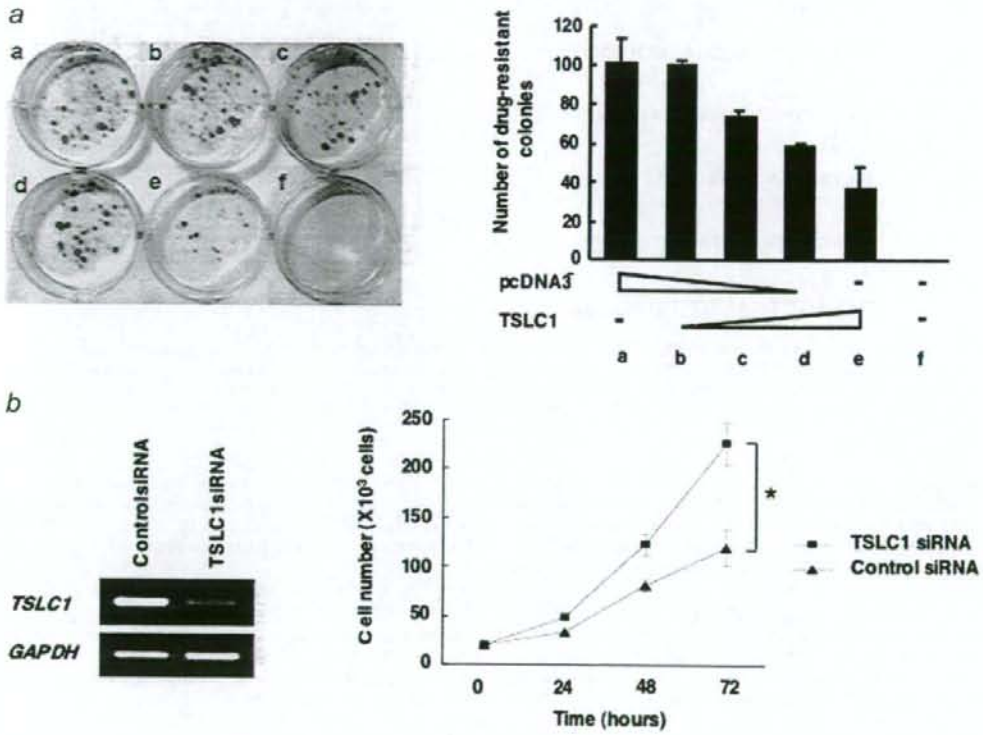

FIGURE 5 – Growth-suppressive potential of TSLC1 in neuroblastoma cells. (*a*) Colony formation assay. SH-SY5Y cells were transfected with the increasing amounts of the expression plasmid for TSLC1 (0, 250, 750 or 1,000 ng). Total amounts of plasmid DNA per transfection were kept constant (1 μg) with pcDNA3. Forty-eight hours after transfection, cells were transferred into the fresh medium containing hygromycin (at a final concentration of 200 μg/ml) and incubated for 2 weeks. Drug-resistant colonies were stained with Giemsa's solution (left panel) and number of drug-resistant colonies was scored (right panel). (*b*) siRNA-mediated knockdown of TSLC1. SH-SY5Y cells were transiently transfected with control siRNA or with siRNA against TSLC1. Forty-eight hours after transfection, total RNA was prepared and subjected to semiquantitative RT-PCR (left panel). At the indicated time periods after transfection, number of viable cells was measured in triplicate (right panel). The differences between the growth rate of control cells and TSLC1-knocked down cells were statistically significant ($p < 0.05$). [Color figure can be viewed in the online issue, which is available at www.interscience.wiley.com.]

Discussion

In the present study, we have demonstrated that the expression levels of a candidate tumor suppressor gene termed *TSLC1* are significantly associated with unfavorable outcome of patients with neuroblastomas. Our array-CGH studies revealed that *TSLC1* gene locates within the SRO of deletion in primary neuroblastoma at 11q. Indeed, its expression levels in primary neuroblastomas correlated with several prognostic indicators for neuroblastoma such as stage, Shimada's pathological classification, *MYCN* amplification status, *TrkA* expression levels and DNA index. Furthermore, TSLC1 had an ability to suppress neuroblastoma cell proliferation. Thus, it is likely that TSLC1 acts as a putative tumor suppressor for neuroblastoma.

As described previously, loss of *TSLC1* expression in primary esophageal squamous cell carcinoma (ESCC) preferentially correlated with invasion and metastasis,[12] and a remarkable reduction of *TSLC1* expression levels was observed in primary lung adenocarcinomas with advanced stage.[13] In addition, *TSLC1* expression was undetectable in 48% of benign (Grade I), 69% of atypical (Grade II) and 85% of anaplastic (Grade III) meningiomas.[14] Consistent with these observations, a significant downregulation of *TSLC1* was seen in unfavorable neuroblastomas bearing *MYCN* amplification as compared with favorable ones carrying single copy of *MYCN*, indicating that the decreased expression levels of *TSLC1* is one of the general properties of various human tumors including neuroblastoma. Intriguingly, there might exist an inverse relationship between the expression levels of *TSLC1* and *MYCN* amplification status in primary neuroblastoma. Indeed, our immunohistochemical analysis demonstrated that TSLC1 is detectable even in unfavorable neuroblastoma without *MYCN* amplification (Case 14). In a sharp contrast to primary neuroblastomas, the expression levels of *TSLC1* might be regulated in a *MYCN*-independent manner in neuroblastoma-derived cell lines. Although the precise molecular mechanisms behind the dysregulated expression of *TSLC1* in neuroblastoma cell lines, it might be due to certain genetic alterations occurred during the establishment of these cell lines.

Based on our present results, the presence of LOH at 11q was associated with unfavorable outcome of patients with neuroblastomas, however, there were no significant correlation between 11q LOH and the decreased expression levels of *TSLC1*. In accordance with these observations, the expression levels of *TSLC1* in neuroblastoma-derived cell lines were independent on their LOH status. These results suggest that the reduced expression levels of *TSLC1* in primary neuroblastomas are not attributed to haploinsufficiency. Alternatively, accumulating evidence strongly suggests that downregulation of *TSLC1* in various cancers including lung cancer, hepatocellular carcinoma, gastric cancer, pancreatic adenocarcinoma, prostate cancer, breast cancer, nasopharyngeal carcinoma and cervical cancer, might be due to the hypermethylation of its promoter region.[9,24–29] In a sharp contrast to these cancers, we did not detect the hypermethylation of the promoter region of *TSLC1* gene in primary neuroblastomas as well as neuroblastoma-derived cell lines under our experimental conditions. During the preparation of our article, Nowacki *et al.* found that there is no *TSLC1*-specific hypermethylation in neuroblastoma.[30] Similarly, the hypermethylation of *TSLC1* promoter region was not detectable in medulloblastoma.[31] According to the previous results, *RASSF1A* and *CASP8* gene promoters were frequently hypermethylated in primary neuroblastoma and neuroblastoma cell lines.[32] Thus, it is conceivable that, unlike the other cancers, hypermethylation of the promoter region of *TSLC1* does not contribute to its downregulation in neuroblastoma, and there might exist as yet unknown tissue-specific regulatory mechanisms of *TSLC1* transcription. Of note, the treatment of neuroblastoma-derived SH-SY5Y and CHP-134 cells with TSA (trichostatin A) resulted in a remarkable upregulation of *TSLC1*. Since TSA is a histone deacetylase inhibitor, it is likely that the acetylation status of histone plays an important role in the regulation of *TSLC1* expression. Further studies should be required to address this issue.

Several lines of evidence indicate that TSLC1 has an ability to delay the cell cycle progression.[12,16,33] Alternatively, enforced expression of TSLC1 resulted in an activation of proapoptotic caspase-3 and induction of proteolytic cleavage of its substrate PARP.[34] These findings strongly suggest that TSLC1 has an antiproliferative and/or proapoptotic activity. In a good agreement with this notion, our present results demonstrated that enforced expression of TSLC1 in SH-SY5Y cells as well as SK-N-AS cells decreases the number of drug-resistant colonies, and enforced depletion of the endogenous TSLC1 in SH-SY5Y cells leads to an accelerated cell proliferation, which was consistent with the recent observations.[30] Collectively, our present findings suggest that TSLC1 acts as a tumor suppressor for neuroblastoma, and also might contribute to the spontaneous regression of neuroblastoma arising from neuronal apoptosis and/or differentiation.

Acknowledgements

We thank institutions and hospitals for providing us tumor specimens. We are grateful to Drs. D.G. Albertson, D. Pinkel, B.G. Feuerstein, N. Tomioka, S. Oba and S. Ishii for their help to array CGH analysis. We also thank Mr. H. Kageyama, Dr. K. Koide, Dr. E. Isogai, Ms. N. Kitabayashi and Ms. Y. Nakamura for their excellent technical assistance. Dr. K. Ando is an awardee of Research Resident Fellowship from the Foundation for Promotion of Cancer Research (Japan) for the 3rd Term Comprehensive 10-Year Strategy for Cancer Control in Japan.

References

1. Evans AE, Gerson J, Schnaufer L. Spontaneous regression of neuroblastoma. Natl Cancer Inst Monogr 1976;44:49–54.
2. Brodeur GM. Neuroblastoma: biological insights into a clinical enigma. Nat Rev Cancer 2003;3:203–16.
3. Tomioka N, Oba S, Ohira M, Misra A, Fridlyand J, Ishii S, Nakamura Y, Isogai E, Hirata T, Yoshida Y, Todo S, Kaneko Y, et al. Novel risk stratification of patients with neuroblastoma by genomic signature which is independent of molecular signature. Oncogene 2008;27:441–9.
4. Guo C, White PS, Weiss MJ, Hogarty MD, Thompson PM, Stram DO, Gerbing R, Matthay KK, Seeger RC, Brodeur GM, Maris JM. Allelic deletion at 11q23 is common in MYCN single copy neuroblastomas. Oncogene 1999;18:4948–57.
5. Attiyeh EF, London WB, Mossé YP, Wang Q, Winter C, Khazi D, McGrady PW, Seeger RC, Look AT, Shimada H, Brodeur GM, Cohn SL, et al. Chromosome 1p and 11q deletions and outcome in neuroblastoma. N Engl J Med 2005;353:2243–53.
6. Mosse Y, Greshock J, King A, Khazi D, Weber BL, Maris JM. Identification and high-resolution mapping of a constitutional 11q deletion in an infant with multifocal neuroblastoma. Lancet Oncol 2003;4:769–71.
7. De Preter K, Vandesompele J, Menten B, Carr P, Fiegler H, Edsjö A, Carter NP, Yigit N, Waelput W, Van Roy N, Bader S, Pahlman S, et al. Positional and functional mapping of a neuroblastoma differentiation gene on chromosome 11. BMC Genomics 2005;6:97.
8. Wang Q, Diskin S, Rappaport E, Attiyeh E, Mosse Y, Shue D, Seiser E, Jagannathan J, Shusterman S, Bansal M, Khazi D, Winter C, et al. Integrative genomics identifies distinct molecular classes of neuroblastoma and shows that multiple genes are targeted by regional alterations in DNA copy number. Cancer Res 2006;66:6050–62.
9. Kuramochi M, Fukuhara H, Nobukuni T, Kanbe T, Maruyama T, Ghosh HP, Pletcher M, Isomura M, Onizuka M, Kitamura T, Sekiya T, Reeves RH, et al. TSLC1 is a tumor suppressor gene in human non-small-cell lung cancer. Nat Genet 2001;27:427–30.
10. Masuda M, Yageta M, Fukuhara H, Kuramochi M, Maruyama T, Nomoto A, Murakami Y. The tumor suppressor protein TSLC1 is involved in cell-cell adhesion. J Biol Chem 2002;277:31014–19.
11. Fukami T, Fukuhara H, Kuramochi M, Maruyama T, Isogai K, Sakamoto M, Takamoto S, Murakami Y. Promoter methylation of TSLC1 gene in advanced lung tumors and various cancer cell lines. Int J Cancer 2003;107:53–9.
12. Ito T, Shimada Y, Hashimoto Y, Kaganoi J, Kan T, Watanabe G, Murakami Y, Imamura M. Involvement of TSLC1 in progression of esophageal squamous cell carcinoma. Cancer Res 2003;653:6320–6.

13. Uchino K, Ito A, Wakayama T, Koma Y, Okada T, Ohbayashi C, Iseki S, Kitamura Y, Tsubota N, Okita Y, Okada M. Clinical implication and prognostic significance of the tumor suppressor TSLC1 gene detected in adenocarcinoma of the lung. Cancer 2003;98:1002–7.
14. Surace EI, Lusis E, Murakami Y, Scheithauer BW, Perry A, Gutmann DH. Loss of tumor suppressor in lung cancer-1 (TSLC1) expression in meningioma correlates with increased malignancy grade and reduced patient survival. J Neuropathol Exp Neurol 2004;63:1015–27.
15. Houshmandi SS, Surace EI, Zhang HB, Fuller GN, Gutmann DH. Tumor suppressor in lung cancer-1 (TSLC1) functions as a glioma tumor suppressor. Neurology 2006;67:1863–6.
16. Lung HL, Cheung AK, Xie D, Cheng Y, Kwong FM, Murakami Y, Guan XY, Sham JS, Chua D, Protopopov AI, Zabarovsky ER, Tsao SW, et al. TSLC1 is a tumor suppressor gene associated with metastasis in nasopharyngeal carcinoma. Cancer Res 2006;66:9385–92.
17. Brodeur GM, Pritchard J, Berthold F, Carlsen NL, Castel V, Castelberry RP, Bernardi BD, Evans AE, Favrot M, Hedborg F. Revisions of the international criteria for neuroblastoma diagnosis, staging, and response to treatment. J Clin Oncol 1993;11:1466–77.
18. Kaneko M, Tsuchida Y, Uchino J, Takeda T, Iwafuchi M, Ohnuma N, Mugishima H, Yokoyama J, Nishihira H, Nakada K, Sasaki S, Sawada T, et al. Treatment results of advanced neuroblastoma with the first Japanese study group protocol. Study Group of Japan for Treatment of Advanced Neuroblastoma. J Pediatr Hematol Oncol 1999;21:190–7.
19. Kaneko M, Nishihira H, Mugishima H, Ohnuma N, Nakada K, Kawa K, Fukuzawa M, Suita S, Sera Y, Tsuchida Y. Stratification of treatment of stage 4 neuroblastoma patients based on N-myc amplification status. Med Pediatr Oncol 1998;31:1–7.
20. Ohira M, Morohashi A, Inuzuka H, Shishikura T, Kawamoto T, Kageyama H, Nakamura Y, Isogai E, Takayasu H, Sakiyama S, Suzuki Y, Sugano S, et al. Expression profiling and characterization of 4200 genes cloned from primary neuroblastomas: identification of 305 genes differentially expressed between favorable and unfavorable subsets. Oncogene 2003;22:5525–36.
21. Misra A, Pellarin M, Shapiro J, Feuerstein BG. A complex rearrangement of chromosome 7 in human astrocytoma. Cancer Genet Cytogenet 2004;151:162–70.
22. Jain AN, Tokuyasu TA, Snijders AM, Segraves R, Albertson DG, Pinkel D. Fully automatic quantification of microarray image data. Genome Res 2002;12:325–32.
23. Kikuchi S, Yamada D, Fukami T, Maruyama T, Ito A, Asamura H, Matsuno Y, Onizuka M, Murakami Y. Hypermethylation of the *TSLC1/IGSF4* promoter is associated with tobacco smoking and a poor prognosis in primary non-small cell lung carcinoma. Cancer 2006;106:1751–8.
24. Fukuhara H, Kuramochi M, Fukami T, Kasahara K, Furuhata M, Nobukuni T, Maruyama T, Isogai K, Sekiya T, Shuin T, Kitamura T, Reeves RH, et al. Promoter methylation of TSLC1 and tumor suppression by its gene product in human prostate cancer. Jpn J Cancer Res 2002;93:605–9.
25. Hui AB, Lo KW, Kwong J, Lam EC, Chan SY, Chow LS, Chan AS, Teo PM, Huang DP. Epigenetic inactivation of TSLC1 gene in nasopharyngeal carcinoma. Mol Carcinog 2003;38:170–8.
26. Honda T, Tamura G, Waki T, Jin Z, Sato K, Motoyama T, Kawata S, Kimura W, Nishizuka S, Murakami Y. Hypermethylation of the TSLC1 gene promoter in primary gastric cancers and gastric cancer cell lines. Jpn J Cancer Res 2002;93:857–60.
27. Steenbergen RD, Kramer D, Braakhuis BJ, Stern PL, Verheijen RH, Meijer CJ, Snijders PJ. TSLC1 gene silencing in cervical cancer cell lines and cervical neoplasia. J Natl Cancer Inst 2004;96:294–305.
28. Jansen M, Fukushima N, Rosty C, Walter K, Altink R, Heek TV, Hruban R, Offerhaus JG, Goggins M. Abberant methylation of 5′ CpG island of TSLC1 is common in pancreatic ductal adenocarcinoma and is first manifest in high-grade PanINs. Cancer Biol Ther 2002;1:293–6.
29. Allinen M, Peri L, Kujala S, Lahti-Domenici J, Outila K, Karppinen SM, Launonen V, Winqvist R. Analysis of 11q21–24 loss of heterozygosity candidate target genes in breast cancer: indications of *TSLC1* promoter hypermethylation. Genes Chromosomes Cancer 2002;34:384–9.
30. Nowacki S, Skowron M, Oberthuer A, Fagin A, Voth H, Brors B, Westermann F, Eggert A, Hero B, Berthold F, Fischer M. Expression of the tumor suppressor gene TSLC1 is associated with favorable outcome and inhibits cell survival in neuroblastoma. Oncogene 2008;27:3329–38.
31. Lindsey JC, Lusher ME, Anderton JA, Bailey S, Gilbertson RJ, Pearson AD, Ellison DW, Clifford SC. Identification of tumor-specific epigenetic in medulloblastoma development by hypermethylation profiling. Carcinogenesis 2004;25:661–8.
32. Lázcoz P, Muñoz J, Nistal M, Pestaña A, Encío I, Castresana JS. Frequent promoter hypermethylation of RASSF1A and CASP8 in neuroblastoma. BMC Cancer 2006;6:254.
33. Sussan TE, Pletcher MT, Murakami Y, Reeves RH. Tumor suppressor in lung cancer 1 (TSLC1) alters tumorigenic growth properties and gene expression. Mol Cancer 2005;4:28.
34. Mao X, Seidlitz E, Truant R, Hitt M, Ghosh HP. Re-expression of TSLC1 in a non-small-cell lung cancer cell line induces apoptosis and inhibits tumor growth. Oncogene 2004;23:5632–42.

THE JOURNAL OF BIOLOGICAL CHEMISTRY VOL. 283, NO. 36, pp. 24426–24434, September 5, 2008

KIF1Bβ Functions as a Haploinsufficient Tumor Suppressor Gene Mapped to Chromosome 1p36.2 by Inducing Apoptotic Cell Death*[S]

Received for publication, March 25, 2008, and in revised form, June 9, 2008 Published, JBC Papers in Press, July 9, 2008, DOI 10.1074/jbc.M802316200

Arasambattu K. Munirajan[‡§¶], Kiyohiro Ando[‡], Akira Mukai[‡], Masato Takahashi[‡], Yusuke Suenaga[‡], Miki Ohira[‡], Tadayuki Koda[§], Toru Hirota[‖], Toshinori Ozaki[‡], and Akira Nakagawara[‡1]

From the [‡]Division of Biochemistry, Chiba Cancer Center Research Institute, Chiba 260-8717, Japan, [§]Research Center for Functional Genomics, Hisamitsu Pharmaceutical Company, Inc., Tokyo 141-8577, Japan, the [¶]Department of Genetics, Dr. ALM PG Institute of Basic Medical Sciences, University of Madras, 600-113 Chennai (Madras), India, and the [‖]Department of Experimental Pathology, The Cancer Institute, Tokyo 135-8550, Japan

Deletion of the distal region of chromosome 1 frequently occurs in a variety of human cancers, including aggressive neuroblastoma. Previously, we have identified a 500-kb homozygously deleted region at chromosome 1p36.2 harboring at least six genes in a neuroblastoma-derived cell line NB1/C201. Among them, only *KIF1Bβ*, a member of the kinesin superfamily proteins, induced apoptotic cell death. These results prompted us to address whether *KIF1Bβ* could be a tumor suppressor gene mapped to chromosome 1p36 in neuroblastoma. Hemizygous deletion of *KIF1Bβ* in primary neuroblastomas was significantly correlated with advanced stages ($p = 0.0013$) and *MYCN* amplification ($p < 0.001$), whereas the mutation rate of the *KIF1Bβ* gene was infrequent. Although *KIF1Bβ* allelic loss was significantly associated with a decrease in *KIF1Bβ* mRNA levels, its promoter region was not hypermethylated. Additionally, expression of *KIF1Bβ* was markedly down-regulated in advanced stages of tumors ($p < 0.001$). Enforced expression of *KIF1Bβ* resulted in an induction of apoptotic cell death in association with an increase in the number of cells entered into the G_2/M phase of the cell cycle, whereas its knockdown by either short interfering RNA or by a genetic suppressor element led to an accelerated cell proliferation or enhanced tumor formation in nude mice, respectively. Furthermore, we demonstrated that the rod region unique to *KIF1Bβ* is critical for the induction of apoptotic cell death in a p53-independent manner. Thus, *KIF1Bβ* may act as a haploinsufficient tumor suppressor, and its allelic loss may be involved in the pathogenesis of neuroblastoma and other cancers.

Neuroblastoma is one of the most common malignant solid tumors occurring in infancy and childhood and accounts for 10% of all pediatric cancers (1). Neuroblastomas are derived from sympathetic neuroblasts with various clinical outcomes from spontaneous regression because of neuronal differentiation and/or apoptotic cell death to malignant progression. Extensive cytogenetic and molecular genetic studies identified that genetic abnormalities such as loss of short arm of chromosome 1 (1p), amplification of *MYCN*, and 17q gain are frequently observed and often associated with poor clinical outcome (2, 3). The actual prevalence of 1p deletion in neuroblastoma is ~35% (4–9). The deleted regions were extensively mapped to identify the candidate tumor suppressor gene(s) that has been deleted out from this region (10–17). A chromosomal locus 1p36 is frequently deleted in aggressive neuroblastoma, pheochromocytoma, colon, liver, brain, breast, and other cancers (18, 19). Transfer of 1p chromosome segments into neuroblastoma-derived cell line NGP.1A.TR1 resulted in a significant suppression of their tumor formation (20). Furthermore, previous studies indicated that there is no single site of deletion on the distal part of 1p36, but there are at least three discrete regions that are commonly deleted in neuroblastoma, indicating that they may harbor potential tumor suppressor gene(s) (8).

Tumor suppressor genes, one of the main classes of cancer-associated genes, encode inhibitors of cell proliferation and/or activators of apoptotic cell death and are involved in a variety of molecular mechanisms behind cell growth suppression (21). Tumor suppressor genes frequently mutated in other malignancies do not appear to play a major role in the generation of neuroblastoma, indicating that development of this type of tumor employs one or more previously unidentified genetic pathways. To date, a majority of candidate tumor suppressor genes has been identified by mapping the minimal deleted region and searching for the intact homologous region of mutated genes. This experimental strategy fails when the second allele is silenced by promoter hypermethylation or the targeted gene is haploinsufficient for tumor suppression, a situation where loss of one allele confers a selective advantage for tumor growth. Several examples of such haploinsufficiency for tumor suppression have been demonstrated in the case of $p27^{KIP1}$, *p53*, and *PTEN* (22, 23).

We and other investigators have previously identified a 500-kb homozygous deletion at 1p36.2 harboring at least six

* This work was supported by the Ministry of Education, Culture, Sports, Science and Technology of Japan and the Ministry of Health, Labor and Welfare of Japan. The costs of publication of this article were defrayed in part by the payment of page charges. This article must therefore be hereby marked "*advertisement*" in accordance with 18 U.S.C. Section 1734 solely to indicate this fact.

[S] The on-line version of this article (available at http://www.jbc.org) contains supplemental Figs. S1–S5.

[1] To whom correspondence should be addressed: Division of Biochemistry, Chiba Cancer Center Research Institute, 666-2 Nitona, Chuo-ku, Chiba 260-8717, Japan. Tel.: 81-43-264-5431; Fax: 81-43-265-4459; E-mail: akiranak@chiba-cc.jp.

genes, *PEX14*, *UFD2a*, *KIF1B*, *CORT*, *DFF45*, and *PGD*, in a neuroblastoma-derived cell line NB1/C201 (12, 15, 24). In this study, we have demonstrated that only *KIF1Bβ*, a member of the kinesin 3 family genes (25), might be a tumor suppressor gene mapped to chromosome 1p36 in neuroblastoma. Kinesins are microtubule-dependent intracellular motors involved in the transport of organelles, vesicles, protein complexes, and RNA to specific destinations (26, 27). *KIF1B* encodes two alternatively spliced isoforms, including *KIF1Bα* and *KIF1Bβ*, and both form homodimers and transport mitochondria and synaptic vesicle precursors, respectively (28). The NH_2-terminal motor domain of *KIF1Bα* is identical to *KIF1Bβ*, whereas COOH-terminal tails share no structural homology. A point mutation in the ATP-binding site within the motor domain of *KIF1Bβ* has been closely linked to Charcot-Marie Tooth disease type 2A (29).

In this study, we cloned a full-length *KIF1Bβ* cDNA, generated recombinant adenovirus encoding *KIF1Bβ*, and examined its biological role in neuroblastoma and other cell lines. We systematically analyzed *KIF1Bβ* for LOH,[2] mutation, and promoter methylation. Our genetic and functional analyses clearly showed that *KIF1Bβ* is a tumor suppressor, although not a classic one. *KIF1Bβ* might act as a haploinsufficient tumor suppressor, and its down-regulation might potentially contribute to tumorigenesis of cancers, including neuroblastoma.

EXPERIMENTAL PROCEDURES

Cell Lines and Tumor Samples—Human neuroblastoma (NB) cell lines such as SH-SY5Y, NB1, and SK-N-BE were grown in RPMI 1640 medium supplemented with heat-inactivated fetal bovine serum, 100 units/ml penicillin, and 100 μg/ml streptomycin. NMuMG, COS7, HEK293, and HeLa cells were grown in Dulbecco's modified Eagle's medium containing 10% heat-inactivated fetal bovine serum, 100 units/ml penicillin, and 100 μg/ml streptomycin. Tumor DNA and RNA samples were obtained from our Neuroblastoma Resource Bank. Informed consent was obtained at each hospital.

GSE-mediated Tumor Formation in Nude Mice—GSE assay was performed as described previously (30). In brief, a cDNA fragment (nucleotide number 2658–3115 of GenBank™ accession number AB017133) corresponding to the unique region of *KIF1Bβ* was amplified by PCR-based strategy and subcloned into the HpaI site of the pLXSN vector in an antisense orientation to give pLXSN-antisense *KIF1Bβ*. NMuMG mammary gland cells (1×10^6 cells) infected with pLXSN or with pLXSN-antisense *KIF1Bβ* were inoculated subcutaneously into the femoral region of nude mice. In the experiments using live animals, we strictly followed the Chiba Cancer Center Research Institute guidelines and protocols for handling live animals.

Construction of Expression Plasmids and Recombinant Adenovirus—*KIF1Bβ* splicing variants I, III, and IV fused to the FLAG epitope at their NH_2 termini were amplified by PCR using cDNA prepared from CHP134 cells as a template and subcloned into pcDNA3.1 (Invitrogen). *KIF1Bβ-GFP* deletion constructs were produced by PCR-based amplification. The recombinant adenovirus was constructed as described previously (31). Briefly, *KIF1Bβ* cDNA was subcloned into pHMCMV6 adeno-shuttle vector. The shuttle vector was then digested with I-CeuI and PI-SceI and inserted into the identical restriction sites of the adenovirus expression vector pAdHM4. All of the recombinant vectors were verified by DNA sequencing. Recombinant adenoviruses were produced by transfecting the PacI-digested expression constructs into HEK293 cells. An expression vector encoding GFP was used to monitor the efficiency of infection.

Mutation Analysis—For the detection of *KIF1Bβ* mutations, we designed primer sets covering the motor domain and 2 kb of the 5′-upstream region of *KIF1Bβ*. After PCR-based amplification, PCR products were separated by 5% nondenaturing polyacrylamide gels. After electrophoresis, PCR products were gel-purified and subcloned into pGEM-T Easy Vector (Promega), and their DNA sequences were determined by an automated DNA sequencer (Applied Biosystems).

Flow Cytometry—Cells were fixed in ice-cold 70% ethanol, treated with 50 mM sodium citrate, 100 μg/ml RNase A, 50 μg/ml propidium iodide and subjected to FACS analysis (BD Biosciences) according to the manufacturer's instructions.

Construction of KIF1Bβ siRNA Expression Vector—An siRNA expression vector termed pMuniH1, in which the cytomegalovirus promoter of pcDNA 3.1 was replaced with the H1 promoter, was generated. Sense and antisense oligonucleotides for *KIF1Bβ* (nucleotide number 371–389 of GenBank™ accession number AB017183) were joined by a 9-base loop, annealed, and subcloned into pMuniH1.

Luciferase Reporter Assay—The genomic fragments corresponding nucleotide positions −887/+106, −630/+106, and −294/+106 of the *KIF1Bβ* gene were amplified from human placenta genomic DNA and cloned into pGL3-Basic luciferase reporter plasmid (Promega) to give pGL3(−887/+106), pGL3(−630/+106), and pGL3(−294/+106). For luciferase assay, SK-N-BE cells were transfected with pRL-TK (Promega) encoding *Renilla* luciferase cDNA and the indicated luciferase reporter constructs. Forty eight hours after transfection, firefly and *Renilla* luciferase activities were measured by dual-luciferase reporter assay system (Promega), and firefly luciferase activity was normalized to *Renilla* luciferase activity.

Methylation-specific PCR—The methylation status of the promoter region of *KIF1Bβ* was assessed by methylation-specific PCR as described previously (32).

Cell Cycle Analysis—Cells were fixed in 3.7% formaldehyde and permeabilized with 0.2% Triton X-100 and DNA was stained with 0.1 μg/ml of 4′,6′-diamidino-2-phenylindole. Cellular DNA content was analyzed by laser scanning cytometry (LSC2 System, Olympus).

Array-CGH Analysis—Array CGH analysis of 112 sporadic primary neuroblastomas using a chip carrying 2,464 bacterial artificial chromosome clones was conducted as described previously (33). All array-CGH data are available at NCBI Gene Expression Omnibus (GEO, www.ncbi.nlm.nih.gov) with accession number GSE 5784.

[2] The abbreviations used are: LOH, loss of heterogeneity; CGH, comparative genomic hybridization; FHA, forkhead-associated; GSE, genetic suppressor element; KIF, kinesin superfamily protein; NB, neuroblastoma; NGF, nerve growth factor; FACS, fluorescence-activated cell sorter; siRNA, short interfering RNA; MTT, 3-(4,5-dimethylthiazol-2-yl)-2,5-diphenyltetrazolium bromide; RT, reverse transcription; GFP, green fluorescent protein.

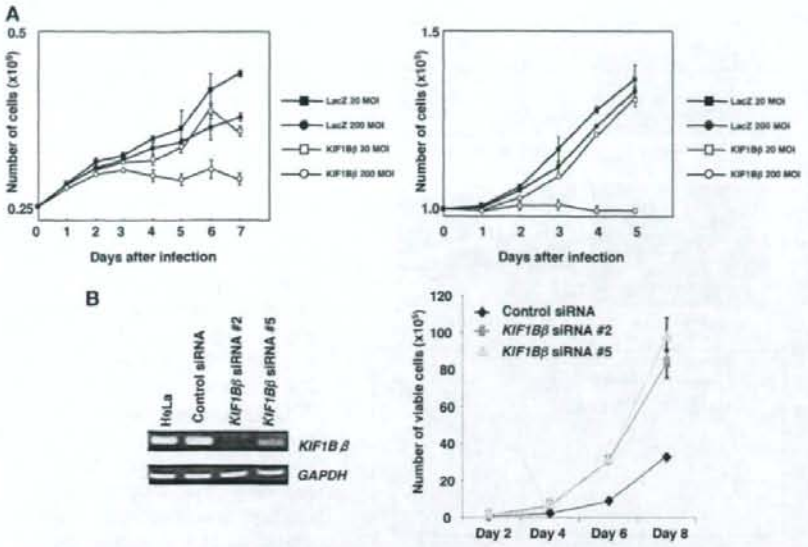

FIGURE 1. ***KIF1Bβ* has a growth-suppressive activity *in vitro*.** *A*, NB1 (*left panel*) and NMuMG (*right panel*) cells were infected with recombinant adenovirus encoding LacZ or *KIF1Bβ* at the indicated multiplicity of infection (*MOI*). At the indicated time points after infection, the number of viable cells was measured. *B*, HeLa cells stably expressing control siRNA-2 or siRNA-5 against *KIF1Bβ* were established, and the expression levels of the endogenous *KIF1Bβ* were examined by RT-PCR (*left panel*). Glyceraldehyde-3-phosphate dehydrogenase (*GAPDH*) was used as an internal control. Number of viable cells was measured at the indicated time points (*right panel*).

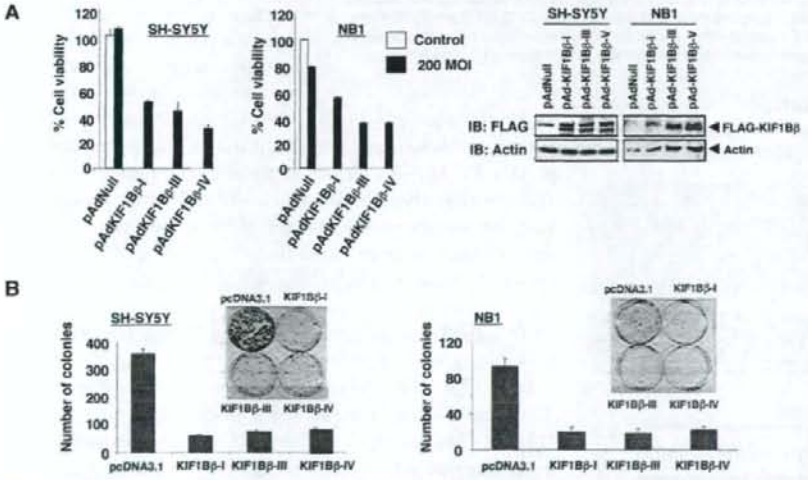

FIGURE 2. **Enforced expression of *KIF1Bβ* induces growth suppression in neuroblastoma-derived cell lines.** *A*, MTT assay. Neuroblastoma-derived SH-SY5Y and NB1 cells were infected with the indicated recombinant adenoviruses, including empty adenovirus (pAdNull) at a 200 multiplicity of infection (*MOI*) (*filled boxes*) or left untreated (*open boxes*). Twenty four hours after infection, infected SH-SY5Y and NB1 cells were seeded at a density of 1×10^3 cells/96-well plates and allowed to attach. Ninety six hours after infection, 10 μl of MTT solution was added to each well and incubated for 3 h at 37 °C (*left panel*). *Right panels* show the expression of the indicated splicing variants of KIF1Bβ as examined by immunoblotting (*IB*) with anti-FLAG antibody. *B*, colony formation assay. SH-SY5Y and NB1 cells were transfected with an empty plasmid or with the indicated expression plasmids. Forty eight hours after transfection, cells were transferred into fresh medium containing 500 μg/ml of G418 and incubated for 2 weeks. After selection with G418, G418-resistant viable colonies were stained with Giemsa solution, and number of colonies was scored.

Caspase Assay—Caspase activity was measured by using caspase-3/7 assay system (Promega) according to the manufacturer's instructions.

Statistics—The Student's *t* test was used as a statistical method. Statistical significance was declared if the *p* value was <0.05.

RESULTS

Identification of KIF1Bβ as a Candidate Tumor Suppressor Mapped to Chromosome 1p36.2—To search for a candidate tumor suppressor gene(s), we first transferred each of the above-mentioned six genes into NB1 and nontransformed NMuMG mouse epithelial cells (30), and we found that only *KIF1Bβ* induces growth suppression in a dose-dependent manner (Fig. 1*A*). In contrast, our preliminary observations indicated that its alternative splicing variant *KIF1Bα* lacking a COOH-terminal rod region has marginal effects on cell growth in NB1 cells (data not shown). In support of these results, siRNA-mediated knockdown of *KIF1Bβ* in HeLa cells without 1p loss markedly enhanced their cell growth (Fig. 1*B*). In addition, enforced expression of *KIF1Bβ* induced growth retardation in *p53*-deficient H1299 cells and HeLa cells in which p53 is inactivated because of the presence of E6-AP (data not shown).

Overexpression of KIF1Bβ in Neuroblastomas-induced Apoptotic Cell Death—During PCR-based screening of human *KIF1Bβ* cDNA from human neuroblastoma cell lines, we identified at least four splicing variants that lacked exons 14 and/or 15 (supplemental Fig. S1). Similar splicing variants have also been observed in mice and rats (34). We successfully generated recombinant adenoviruses for human KIF1Bβ-I, -III, and -IV variants (Fig. 2*A*). Enforced expression of these splicing variants promoted apoptotic cell death in both SH-SY5Y (without 1p loss) and NB1 neuroblastoma cell lines as determined by MTT and FACS analyses (Fig. 2*A* and supplemental Fig. S2). Consistent with these results, colony formation assay showed that all these KIF1Bβ splicing variants strongly reduced the number of drug-resistant colonies in SH-SY5Y and NB1 neuroblastoma cells (Fig. 2*B*). These findings suggest that multiple KIF1Bβ splicing isoforms

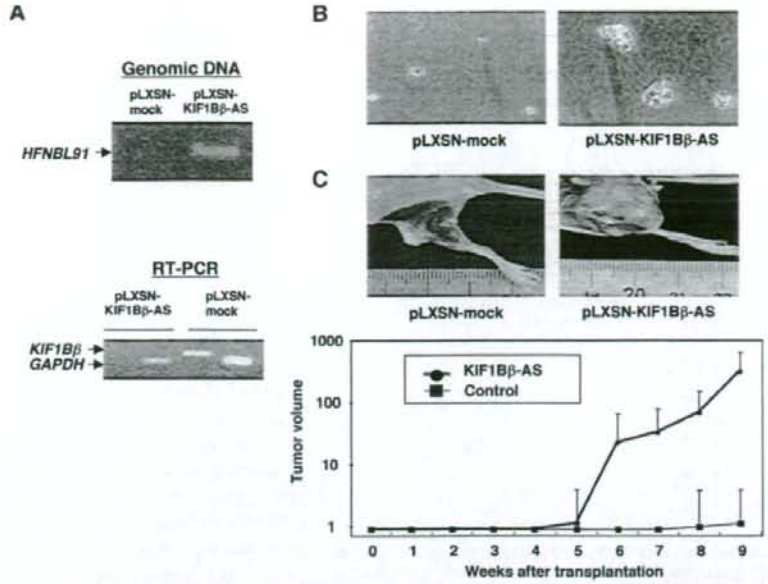

FIGURE 3. **Tumor formation *in vivo*.** *A*, NMuMG cells were infected with an empty retrovirus vector (pLXSN) or with pLXSN bearing mouse antisense *KIF1Bβ* (pLXSN-*KIF1Bβ*-AS). Genomic integration of the antisense *KIF1Bβ* was examined by PCR (*upper panel*). *Lower panel* shows the expression levels of *KIF1Bβ* as examined by RT-PCR. *Arrows* indicate the positions of PCR products corresponding to *KIF1Bβ* and *GAPDH*. *B*, NMuMG cells (5×10^4 cells) infected with pLXSN or pLXSN-KIF1Bβ-AS were suspended in 3 ml of 0.4% low melting agarose dissolved in culture medium, plated onto agarose bed consisting of 0.8% low-melting agarose, and incubated at 37 °C for 5 weeks. *C*, tumor formation in nude mice. NMuMG cells (1×10^6 cells) infected with the indicated retroviruses were injected subcutaneously and tumor volumes were estimated weekly (*lower panel*). *Upper panels* show tumors generated in nude mice.

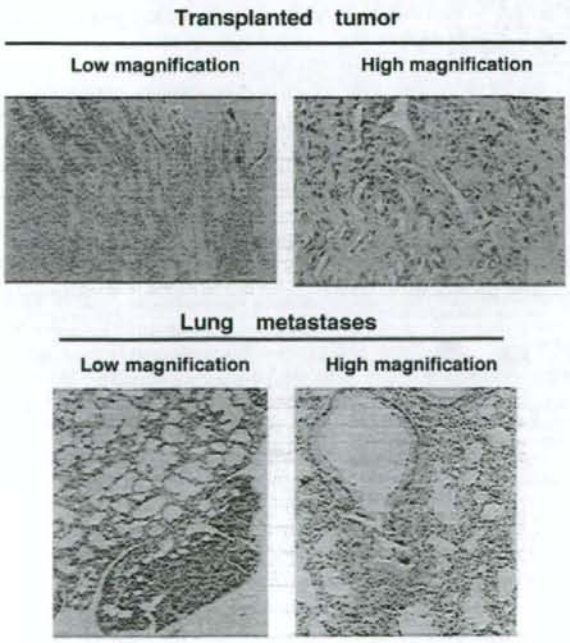

FIGURE 4. **Histology of tumors generated in nude mice.** Representative photographs of tumors (*upper panels*) and lung metastasis (*lower panels*) are shown. For histological analyses, tumor tissues were removed from animals and immediately fixed in 10% formaldehyde and embedded in paraffin, and 3-μm sections were stained with hematoxylin and eosin.

possess tumor suppressor activity. Intriguingly, the expression pattern of *KIF1Bβ* splicing variants was varied among various human tissues (supplemental Fig. S3).

Knockdown of KIF1Bβ Expression Accelerates Growth of NMuMG Cells and Tumor Formation in Nude Mice—We then asked whether genetic disruption of *KIF1Bβ* gene could be critical for tumorigenesis. For this purpose, we employed a genetic suppressor element (GSE) strategy (30). A mouse genomic DNA corresponding to a *KIF1Bβ* cDNA fragment (nucleotide number 2658–3115 of GenBank™ accession number AB017133) encoding the unique region of *KIF1Bβ* was subcloned into the retrovirus pLXSN vector in an antisense orientation to give pLXSN-KIF1Bβ-AS. NMuMG cells, immortalized mouse mammary gland cells, stably infected with pLXSN-KIF1Bβ-AS, showed more than 80% reduction in endogenous *KIF1Bβ* expression (Fig. 3*A*) and formed significantly larger colonies than empty vector-infected control cells in soft agar medium (Fig. 3*B*). In addition, all eight mice subcutaneously transplanted with NMuMG cells stably infected with pLXSN-KIF1Bβ-AS displayed remarkable tumor growth (Fig. 3*C*). On the other hand, only two of eight mice transplanted with the empty vector-infected cells formed tumors, which were smaller in both cases (note log scale in Fig. 3*C*). The tumors formed by cells lacking *KIF1Bβ* expression were histologically diagnosed as poorly differentiated invasive ductal carcinoma and frequently metastasized to the lung (Fig. 4). Thus, it is likely that KIF1Bβ exerts tumor-suppressive function *in vivo*.

LOH of KIF1Bβ Locus Is Frequently Observed in Primary Advanced Neuroblastomas—We next sought to search for LOH at chromosome 1p36 in 112 sporadic neuroblastomas using array-based comparative genomic hybridization (array-CGH). Similar to previous reports, the smallest region of overlap at the distal region of chromosome 1p identified in 37 primary neuroblastomas with 1p loss was between 1p36.22 and 1pter and included *KIF1B*, *CHD5*, *TP73*, and *SKI* (supplemental Fig. S4). Thirty two percent (30/95) of neuroblastomas examined had lost one *KIF1Bβ* allele as determined by quantitative real time genomic PCR (Table 1). *KIF1Bβ* was hemizygously deleted in 18% of early neuroblastomas (stages 1 and 2, $n = 51$), in 55% of advanced neuroblastomas (stages 3 and 4, $n = 38$) ($p = 0.0013$), in 13% of primary neuroblastomas with a single copy of *MYCN* ($n = 70$), and in 84% of *MYCN*-amplified primary neuroblastomas ($n = 25$) ($p < 0.001$). No homozygous deletion was detected in the primary tumors examined.

Decreased Expression of KIF1Bβ Is Associated with Monoallelic Loss of the Gene in Primary Neuroblastomas—We examined expression levels of *KIF1Bβ* mRNA in 102 primary neuroblastomas by using both semi-quantitative and quantitative real time PCRs. As shown in Fig. 5, *A* and *B*, expression levels of *KIF1Bβ* mRNA were significantly higher in tumors at favorable stages (1, 2, and 4s, 1.654 ± 0.257, mean ± S.E., $n = 60$) than in those at advanced stages (3 and 4, 0.503 ± 0.180, $n = 42$, $p < 0.001$). To address whether its expression levels could be correlated with number of alleles at the *KIF1Bβ* gene locus, we examined primary tumors with a diploid karyotype. As shown in the *lower panel* of Fig. 5*B*, tumors with monoallelic loss of *KIF1Bβ* gene locus expressed significantly lower levels of *KIF1Bβ* mRNA (0.126 ± 0.092, $n = 13$) as compared with those with two *KIF1Bβ* alleles (0.364 ± 0.035, $n = 16$, $p = 0.019$). These results suggest that *KIF1Bβ* is a haploinsufficient tumor suppressor gene in high risk neuroblastomas.

TABLE 1

Frequency of LOH of the *KIF1B* gene

LOH was examined by both array-CGH and quantitative real time PCR using genomic DNA obtained from primary neuroblastomas (tumor cells component, >70%). The cutoff value of the LOH score was 0.8 in the latter.

Category	*n*	*KIF1B* LOH	
		LOH (+)	%
Stage			
1	36	6	17
2	15	3	20
3	7	3	43
4	31	18	58
4s	6	0	0
MYCN			
Single copy	70	9	13
Amplification	25	21	84
Total	95	30	32

No Promoter Methylation and Rare Mutations Are Observed in Neuroblastoma Cell Lines and Primary Neuroblastomas—Our initial mutation searches of *KIF1Bβ* gene were focused on its motor domain and the proximal (~2 kb) promoter region in 21 primary neuroblastomas with 1p36 LOH and in 17 neuroblastoma cell lines. As shown in Table 2, we identified only a silent mutation GCC-GCG (at codon 95) in two primary tumors, a 2-bp (CC) deletion (at −113/−114) and G-A base change (at −336) in the *KIF1Bβ* promoter region in three primary tumors and four neuroblastoma cell lines. Because these aberrations were also found in the control samples, it is likely that these base changes reflect single nucleotide polymorphisms of the Japanese population.

To further extend our mutation searches, we have examined the presence or absence of *KIF1Bβ* mutations within its whole coding region in 100 primary neuroblastoma tissues. Finally, we found out the missense mutations (N737S) in six independent cases. However, their functional significances remained unclear.

Methylation of CpG islands in the promoters has been considered to be another well recognized molecular mechanism behind the inactivation of the tumor suppressor gene. To determine whether the methylation of CpG island could contribute to the inactivation of *KIF1Bβ*, the region spanning exon 1 and 5′-upstream sequences (nucleotide number −877 to +106) of *KIF1Bβ* was cloned and analyzed for promoter activity by luciferase reporter assay. As shown in Fig. 6, *A* and *B*, *KIF1Bβ* promoter region existed at nucleotide position between −630 and −294. We then identified *KIF1Bβ* CpG islands within the promoter region and investigated whether these CpGs could be methylated in primary neuroblastomas as well as cell lines. The methylation-specific PCR analysis demonstrated that all of the CpG clusters are unmethylated, suggesting that *KIF1Bβ* is not inactivated by methylation (Fig. 6*C*).

The COOH-terminal Region between FHA and Pleckstrin Homology Domains of KIF1Bβ Is Responsible to Induce Apoptotic Cell Death—To map a critical domain(s) of KIF1Bβ responsible for its tumor-suppressive function, we generated NH_2-

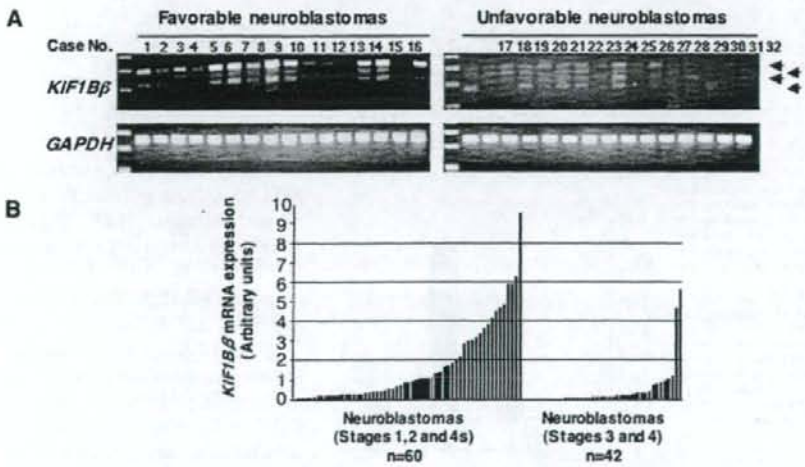

KIF1Bβ alleles	Number of diploid tumours	*KIF1Bβ* expression (Mean±SEM)	*P*-value
Mono-allelic	13	0.126 ± 0.092	0.019
Bi-allelic	16	0.364 ± 0.035	

FIGURE 5. **Expression levels of *KIF1Bβ* in primary neuroblastomas.** *A*, semi-quantitative RT-PCR analysis. Total RNA was prepared from favorable ($n = 16$; stages 1 and 2, *MYCN* single copy) and unfavorable ($n = 16$; stages 3 and 4, *MYCN* amplified) neuroblastomas and subjected to semi-quantitative RT-PCR to examine the expression levels of *KIF1Bβ*. Glyceraldehyde-3-phosphate dehydrogenase (*GAPDH*) was used as an internal control. *B*, quantitative real time PCR. Expression levels of *KIF1Bβ* were standardized using the corresponding glyceraldehyde-3-phosphate dehydrogenase value of each neuroblastoma sample. The relative expression levels of *KIF1Bβ* in favorable (stages 1, 2,and 4s) and advanced (stages 3 and 4) neuroblastomas are shown (*upper panel*). *Lower panel* shows a significant correlation between mono-allelic loss of *KIF1Bβ* gene and its lower expression levels.

TABLE 2
Mutation analyses of *KIF1Bβ* gene

S. no.	Case no.	Exon 4–6	KIF exon 15	KIF promotor F12	KIF promotor F11	F/UF[a]
1	NB-1					NA
2	NB-2		G→A	Δ2 bp (−113–4)	G→A (−366)	NA
3	NB-3					UF
4	NB-4		G→A			UF
5	NB-5		/			NA
6	NB-6	GCC/GCG (95)	/	Δ2 bp (−113–4)	G→A (−366)	F
7	NB-7		/			UF
8	NB-8		/			UF
9	NB-9		/			F
10	NB-10		/			F
11	NB-11		/			UF
12	NB-12		/			UF
13	NB-13	GCC/GCG (95)	/	Δ2 bp (−113–4)	G→A (−366)	UF
14	NB-14		/			NA
15	NB-15		/			NA
16	NB-16		/			NA
17	NB-17		/			NA
18	NB-18		/			NA
19	NB-19		/			UF
20	NB-20		/			NA
21	NB-21		/			F
22	NB-GAMB		G>A	Δ2 bp (−113–4)	G→A (−366)	Cell line
23	NB-GOTO/P3					Cell line
24	NB-KAN		G>A	Δ2 bp (−113–4)	G→A (−366)	Cell line
25	NB-LHN		G>A	Δ2 bp (−113–4)	G→A (−366)	Cell line
26	NB-NB9					Cell line
27	NB-NB69		/			Cell line
28	NB-NBLS		/			Cell line
29	NB-NBTu-1		/			Cell line
30	NB-NLF		/			Cell line
31	NB-NMB		/	Δ2 bp (−113–4)	G→A (−366)	Cell line
32	NB-OAN		/			Cell line
33	NB-SK-N-AS		/			Cell line
34	NB-SK-N-BE		/			Cell line
35	NB-SK-N-SH		/			Cell line
36	NB-SH-SY5Y		/			Cell line
37	NB-CHP134		/			Cell line
38	NB-TGW	GCC/GCG (95)	/			Cell line

[a] For Shimada classification, F indicates favorable histology; UF indicates unfavorable histology, and NA indicates not analyzed.

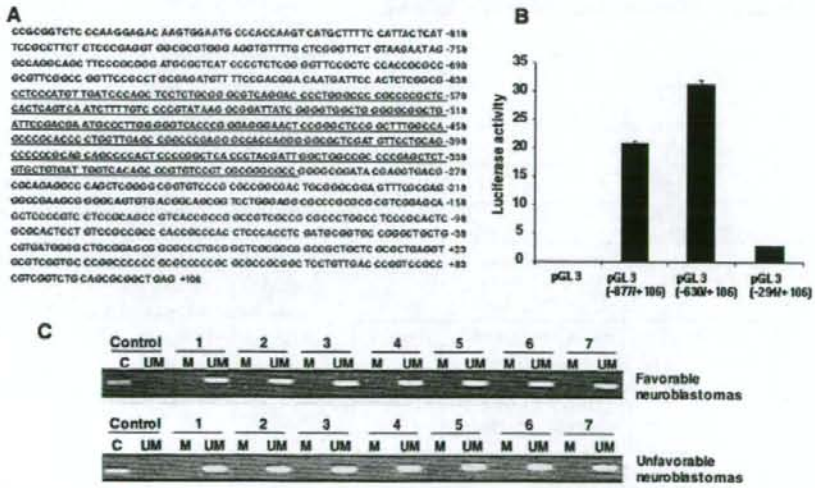

FIGURE 6. **Identification of the promoter region of human *KIF1Bβ* gene and its methylation status.** *A*, nucleotide sequence of 5′-upstream region and a part of exon 1 of human *KIF1Bβ* gene. +1 indicates the first nucleotide of exon 1. CpG island is indicated by *underline*. *B*, luciferase reporter assay. Neuroblastoma-derived SK-N-BE cells were transiently co-transfected with the constant amount of pRL-TK encoding *Renilla* luciferase cDNA and the indicated luciferase reporter constructs. Forty eight hours after transfection, cells were lysed, and their luciferase activities were measured. *C*, methylation-specific PCR. Methylation status of the promoter region of *KIF1Bβ* gene in primary neuroblastomas was examined by methylation-specific PCR. *M*, methylated; *UM*, unmethylated; *C*, control.

terminal deletion mutants of KIF1Bβ splicing isoform IV lacking motor domain (KIF1Bβ-IV-Del 1-GFP), motor and FHA domains (KIF1Bβ-IV-Del 2-GFP), coiled-coil domain (KIF1Bβ-IV-Del 3-GFP), and FHA and coiled-coil domains (KIF1Bβ-IV-Del 4-GFP) fused with enhanced green fluorescent protein at their COOH termini (Fig. 7*A*). COS7 cells were transfected with wild-type or with KIF1Bβ-IV-Del-GFP fusion constructs and followed by live confocal laser scanning microscopy. Forty eight hours after transfection, KIF1Bβ-GFP-positive cells began to lose their normal cell morphology. Seventy two hours after transfection, most of the cells underwent apoptotic cell death and detached from the cell culture dish (Fig. 7, *B* and *D*). Expression of splicing variants-I, -III, and -IV along with deletion mutants of splicing variant-IV lacking the motor

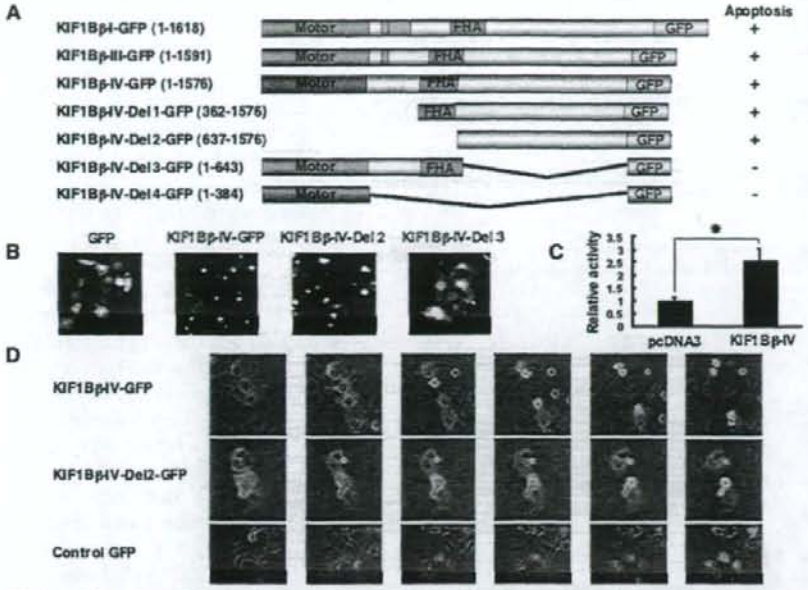

FIGURE 7. **The coiled-coil region is required for *KIF1Bβ*-mediated apoptotic cell death.** *A*, schematic representation of GFP-tagged KIF1Bβ deletion mutants and summary of their ability to induce apoptotic cell death. *B*, COS7 cells were transiently transfected with the indicated expression plasmids. Forty eight hours after transfection, morphologies of GFP-positive cells were examined by a confocal laser scanning microscope. *C*, caspase activity. HeLa cells were transiently transfected with the indicated expression plasmids. Forty eight hours after transfection, cell lysates were prepared, and their caspase activities were measured. Statistically significant differences are indicated by *asterisks* ($p < 0.05$). *D*, time course experiments. The indicated expression plasmids were transiently introduced into COS7 cells. Forty eight hours after transfection, changes of morphology of GFP-positive cells were monitored for 12 h.

domain (with or without FHA domain) also induced apoptotic cell death. In contrast, expression of KIF1Bβ mutants lacking the COOH-terminal rod domain did not promote apoptotic cell death (Fig. 7, *A* and *B*). Under our experimental conditions, enforced expression of KIF1Bβ variant-IV resulted in a significant increase in the caspase activities (Fig. 7*C*), suggesting that KIF1Bβ-mediated apoptotic cell death might be regulated in a caspase-dependent manner. Our further analysis using other deletion mutants revealed that the 807 amino acids death-inducing region is located between FHA and pleckstrin homology domains (data not shown).

To determine whether the kinesin activity of KIF1Bβ could be necessary for its tumor-suppressive function, we introduced a Q98L mutation within a consensus ATP-binding site of KIF1Bβ-IV splicing variant (Fig. 8*A*). This mutation disrupts the motor function of KIF1Bβ (29). In addition, a KIF1Bβ-IV splicing variant carrying two point mutations (Q560A and D568A) within its highly conserved amino acid residues of FHA domain, which may be critical for binding to Ser/Thr-phosphorylated motifs of the interacting proteins, was also generated. In addition to these two mutants, we also generated an additional mutant bearing Q98L, Q560A, and D568A. These three mutants, however, retained an ability to induce apoptotic cell death, suggesting that KIF1Bβ-mediated apoptotic cell death does not require its ability to transport cargo using its motor domain (Fig. 8*B*).

DISCUSSION

In this study, we have shown that the *KIF1Bβ* gene is hemizygously deleted especially in aggressive primary neuroblastoma tumors, and its mutation is infrequent. The expression of *KIF1Bβ* was kept at quite a low level in aggressive neuroblastoma subsets, even though no methylation of its promoter region was observed. One of the well known haploinsufficient tumor suppressors is the cyclin-dependent kinase inhibitor $p27^{KIP1}$ (35). The heterozygous mice of $p27^{KIP1}$ developed tumors when mice were treated with tumor-promoting agents, and tumors retained the normal $p27^{KIP1}$ allele. Additionally, hemizygous loss of $p27^{KIP1}$ and/or reduced expression level of $p27^{KIP1}$ conferred poor prognosis in human cancers (36). Taken together, our present results suggest that, like $p27^{KIP1}$, *KIF1Bβ* is a haploinsufficient tumor suppressor gene of neuroblastoma, and its function to induce apoptotic cell death is regulated in a p53-independent manner. Although homozygous deletion or mutations of *KIF1Bβ* were rarely detectable in this study, several losses of function mutations in the coding region of *KIF1Bβ* gene in a large number of primary neuroblastomas, pheochromocytomas, and medulloblastomas have now been identified.[3] Homozygous deletion of *KIF1B* in mice resulted in death just after birth because of apnea. However, heterozygous mice are viable with a phenotype resembling Charcot-Marie-Tooth disease type 2A (29). To date, no information has been available in the literature regarding spontaneous tumor formation in *KIF1B*-heterozygous mice. It is possible that these mice have not been followed long enough or that loss of one *KIF1B* allele is not sufficient for tumor formation and requires cooperating mutations for spontaneous tumor formation. Since there is functional disruption of wild-type p53 because of its mislocalization, haploinsufficiency of the *KIF1Bβ* gene might contribute to tumorigenesis of aggressive neuroblastomas with 1p LOH and *MYCN* amplification (37). *KIF1Bβ* might also be involved in tumorigenesis in combination with other contiguous 1p36.3 genes such as *p73* (38) and *CHD5* (39).

Finally, we have identified four different splicing variants of KIF1Bβ. However, colony formation assay revealed that all of the splicing variants almost equally suppress cell growth, indicating that its tumor-suppressive function may not be dependent on alternative splicing events. The deletion construct termed Del 2-GFP encoding amino acid residues 637–1576

[3] S. Schlisio and W. G. Kaelin, Jr., personal communication.

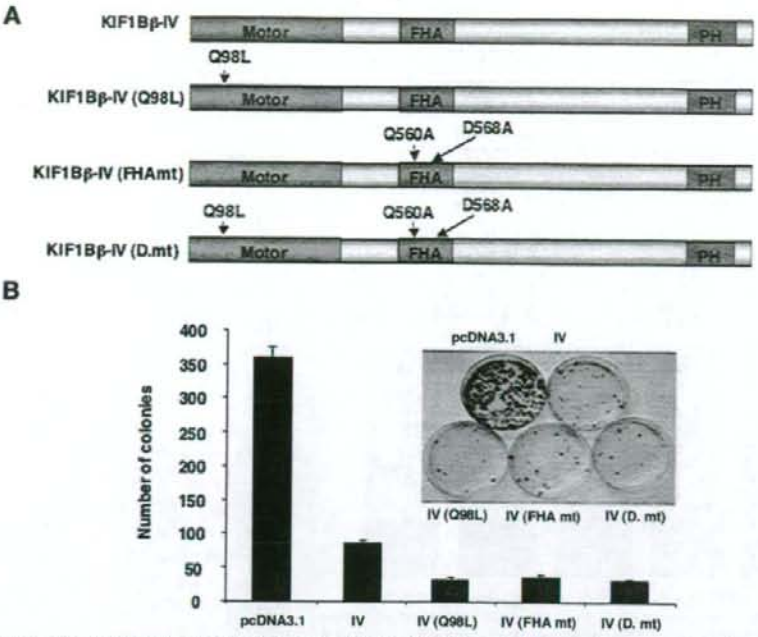

FIGURE 8. **Motor and FHA domains are not required for *KIF1Bβ*-mediated growth suppression.** *A*, schematic drawing of mutant forms of KIF1Bβ. Point mutations (Q98L, Q560A, and D568A) were introduced into *KIF1Bβ* by using the QuickChange XL site-directed mutagenesis kit (Stratagene) following the manufacturer's recommendations. *B*, colony formation assay. SH-SY5Y cells were transfected with an empty vector or with the indicated expression vectors. Forty eight hours after transfection, cells were transferred into fresh medium containing 500 μg/ml of G418. Two weeks after selection, G418-resistant colonies were fixed and stained with Giemsa solution, and number of drug-resistant colonies was scored.

induced apoptotic cell death similar to wild-type KIF1Bβ. Therefore, this region containing two predicted coiled-coils (amino acid residues 668–737 and 841–863) alone is sufficient for pro-apoptotic function of KIF1Bβ. The coiled-coil motifs are amphipathic oligomerization motifs. The tumor suppressor par-4 with a potential coiled-coil structure induced apoptotic cell death in prostate cancer cell lines (40, 41). Moreover, a putative coiled-coil domain of potential tumor suppressor protein, Prohibitin, has been shown to be sufficient to repress E2F1-mediated transcription and induction of apoptotic cell death (42).

In neuroblastoma, polyploidy is very common, which is often associated with a better prognosis. The precise molecular mechanisms underlying this phenomenon still remain unclear. Recently, defects in mitotic spindle check point gene products such as MAD1, MAD2, BUB1, BUB3, and BUBR1 have been implicated in the generation of polyploidy (43). Intriguingly, attached cells expressing GFP-tagged KIF1Bβ splicing variants exhibited a perturbation of G_2/M progression and multinucleation (supplemental Fig. S5). The precise molecular mechanisms by which KIF1Bβ could promote these cellular abnormalities and apoptotic cell death are currently unknown. On the other hand, down-regulation of KIF1Bβ resulted in augmented cell proliferation *in vitro* and tumor formation *in vivo*, indicating that KIF1Bβ might have a critical role in the regulation of mitosis like other mitotic kinesins (44). It is conceivable that KIF1Bβ might act in a dominant inhibitory manner to sequester fundamental cytoplasmic factors that are required for proper cell cycle progression. In this connection, we are undertaking to identify the KIF1Bβ-binding partner(s), which might clarify the molecular mechanisms behind growth suppression and/or apoptotic cell death mediated by KIF1Bβ.

The nerve growth factor (NGF) dependence of tumor cells through the TrkA-p75^{NTR} receptor complex plays a critical role in the regulation of the spontaneous regression and differentiation in neuroblastoma (45). NGF depletion-induced apoptotic cell death is blocked in aggressive neuroblastoma (46). The findings showing that expression of *KIF1Bβ* also increases during apoptotic cell death triggered by NGF depletion in PC12 cells[3] strengthen the significance of the tumor suppressor function of KIF1Bβ in primary neuroblastomas and pheochromocytoma. Indeed, some kinesin family proteins are involved in the regulation of apoptotic cell death in developing neurons (47). In conclusion, our present results unveiled that *KIF1Bβ*, mapped to chromosome 1p36.2, is the candidate tumor suppressor gene of the kinesin family functioning in a manner of haploinsufficiency.

Acknowledgments—We thank Hajime Kageyama for help in FACS analysis and DNA sequencing; Yuki Nakamura, Natsue Kitabayashi, and Ayaka Nobusato for their excellent technical assistance; Drs. Keizo Takenaga, Kou Miyazaki, Hisashi Tokita, Nobumoto Tomioka, Yoko Nakamura, and Daihachiro Tomotsune for helpful discussions; and Drs. E. Thavathiru and Margaret Das for critical reading of the manuscript.

REFERENCES

1. Westemann, F., and Schwab, M. (2002) *Cancer Lett.* **184,** 127–147
2. Brodeur, G. M., Seeger, R. C., Schwab, M., Varmus, H. E., and Bishop, J. M. (1984) *Science* **224,** 1121–1124
3. Caron, H. (1995) *Med. Pediatr. Oncol.* **24,** 215–221
4. Gehring, M., Berthold, R., Edler, L., Schwab, M., and Amler, L. C. (1995) *Cancer Res.* **55,** 5366–5369
5. White, P. S., Maris, J. M., Beltinger, C., Sulman, E., Marshall, H. N., Fujimori, M., Kaufman, B. A., Biegel, J. A., Allen, C., Hilliard, C., Valentine, M. B., Look, A. T., Enomoto, H., Sakiyama, S., and Brodeur, G. M. (1995) *Proc. Natl. Acad. Sci. U. S. A.* **92,** 5520–5524
6. Martinsson, T., Sjoberg, R. M., Hedborg, F., and Kongner, P. (1995) *Cancer Res.* **55,** 5681–5686
7. White, P. S., Thompson, P. M., Seifried, B. A., Sulman, E. P., Jensen, S. J., Guo, C., Maris, J. M., Hogarty, M. D., Allen, C., Biegel, J. A., Matise, T. C., Gregory, S. G., Reynolds, C. P., and Brodeur, G. M. (2001) *Med. Pediatr. Oncol.* **36,** 37–41

8. Brodeur, G. M. (2003) *Nat. Rev. Cancer* **3,** 203–216
9. White, P. S., Thompson, P. M., Gotoh, T., Okawa, E. R., Igarashi, J., Kok, M., Winter, C., Gregory, S. G., Hogarty, M. D., Maris, J. M., and Brodeur, G. M. (2005) *Oncogene* **24,** 2684–2694
10. Hogarty, M. D., Liu, X., Guo, C., Thompson, P. M., Weiss, M. J., White, P. S., Sulman, E. P., Brodeur, G. M., and Maris, J. M. (2000) *Med. Pediatr. Oncol.* **6,** 512–515
11. Nakagawara, A., Ohira, M., Kageyama, H., Mihara, M., Furuta, S., Machida, T., Takayasu, H., Islam, A., Nakamura, Y., Takahashi, M., Shishikura, T., Kaneko, Y., Toyoda, A., Hattori, M., Sakaki, Y., Ohki, M., Horii, A., Soeda, E., Inazawa, J., Seki, N., Kuma, H., Nozawa, I., and Sakiyama, S. (2000) *Med. Pediatr. Oncol.* **35,** 516–521
12. Ohira, M., Kageyama, H., Mihara, M., Furuta, S., Machida, T., Shishikura, T., Takayasu, H., Islam, A., Nakamura, Y., Takahashi, M., Tomioka, N., Sakiyama, S., Kaneko, Y., Toyoda, A., Hattori, M., Sakaki, Y., Ohki, M., Horii, A., Soeda, E., Inazawa, J., Seki, N., Kuma, H., Nozawa, I., and Nakagawara, A. (2000) *Oncogene* **19,** 4302–4307
13. Bauer, A., Savelveva, L., Claas, A., Praml, C., Berthold, F., and Schwab, M. (2001) *Genes Chromosomes Cancer* **31,** 228–239
14. Caron, H., Spieker, N., Godfried, M., Veenstra, M., van Sluis, P., de Kraker, J., Voûte, P., and Versteeg, R. (2001) *Genes Chromosomes Cancer* **30,** 168–174
15. Chen, Y. Z., Soeda, E., Yang, H. W., Takita, J., Chai, L., Horii, A., Inazawa, J., Ohki, M., and Hayashi, Y. (2001) *Genes Chromosomes Cancer* **31,** 326–332
16. Ejeskar, K., Sjoberg, R. M., Abel, F., Kogner, P., Ambros, P. F., and Martinsson, T. (2001) *Med. Pediatr. Oncol.* **36,** 61–66
17. Mosse, Y. P., Greshock, J., Margolin, A., Naylor, T., Cole, K., Khazi, D., Hii, G., Winter, C., Shahzad, S., Asziz, M. U., Biegel, J. A., Weber, B. L., and Maris, J. M. (2005) *Genes Chromosomes Cancer* **43,** 390–403
18. Schwab, M., Praml, C., and Amler, L. C. (1996) *Genes Chromosomes Cancer* **16,** 211–229
19. Schwab, M., Westermann, F., Hero, B., and Berthold, F. (2003) *Lancet* **4,** 472–480
20. Bader, S. A., Fasching, C., Brodeur, G. M., and Stanbridge, E. J. (1991) *Cell Growth & Differ.* **5,** 245–255
21. Sherr, C. J. (2004) *Cell* **116,** 235–246
22. Cook, W. D., and McCaw, B. J. (2000) *Oncogene* **19,** 3434–3438
23. Fodde, R., and Smits, R. (2002) *Science* **298,** 761–763
24. Nagai, M., Ichimiya, S., Ozaki, T., Seki, N., Mihara, M., Furuta, S., Ohira, M., Tomioka, N., Nomura, N., Sakiyama, S., Kubo, O., Takakura, K., Hori, T., and Nakagawara, A. (2000) *Int. J. Oncol.* **16,** 907–916
25. Lawrence, C. J., Dawe, R. K., Christie, K. R., Cleveland, D. W., Dawson, S. C., Endow, S. A., Goldstein, L. S., Goodson, H. V., Hirokawa, N., Howard, J., Malmberg, R. L., McIntosh, J. R., Miki, H., Mitchison, T. J., Okada, Y., Reddy, A. S., Saxton, W. M., Schliwa, M., Scholey, J. M., Vale, R. D., Walczak, C. E., and Wordeman, L. (2004) *J. Cell Biol.* **167,** 19–22
26. Hirokawa, N. (1998) *Science* **279,** 519–526
27. Goldstein, L. S., and Philp, A. V. (1999) *Annu. Rev. Cell Dev. Biol.* **15,** 141–183
28. Nangaku, M., Sato-Yoshitake, R., Okada, Y., Noda, Y., Takemura, R., Yamazaki, H., and Hirokawa, N. (1994) *Cell* **79,** 1209–1220
29. Zhao, C., Takita, J., Tanaka, Y., Setou, M., Nakagawa, T., Takeda, S., Yang, H. W., Terada, S., Nakata, T., Takei, Y., Saito, M., Tsuji, S., Hayashi, Y., and Hirokawa, N. (2001) *Cell* **105,** 587–597
30. Garkavtsev, I., Kazarov, A., Gudkov, A., and Riabowol, K. (1996) *Nat. Genet.* **14,** 415–420
31. Mizuguchi, H., and Kay, M. A. (1998) *Hum. Gene Ther.* **9,** 2577–2583
32. Herman, J. G., Graff, J. R., Myohansen, S., Nelkin, B. D., and Baylin, S. B. (1996) *Proc. Natl. Acad. Sci. U. S. A.* **93,** 9821–9826
33. Tomioka, N., Oba, S., Ohira, M., Misra, A., Fridlyand, J., Ishii, S., Nakamura, Y., Isogai, E., Hirata, T., Yoshida, Y., Todo, S., Kaneko, Y., Albertson, D. G., Pinkel, D., Feuerstein, B. G., and Nakagawara, A. (2008) *Oncogene* **27,** 441–449
34. Gong, T. W., Winnicki, R. S., Kohrman, D. C., and Lomax, M. I. (1999) *Gene (Amst.)* **239,** 117–127
35. Fero, M. L., Randel, E., Gurley, K. E., Roberts, J. M., and Kemp, C. J. (1998) *Nature* **396,** 177–180
36. Blain, S. W., Scher, H. I., Cordon-Cardo, C., and Koff, A. (2003) *Cancer Cell* **3,** 111–115
37. Moll, U. M., LaQuaglia, M., Benard, J., and Riou, G. (1995) *Proc. Natl. Acad. Sci. U. S. A.* **92,** 4407–4411
38. Ichimiya, S., Nimura, Y., Kageyama, H., Takada, N., Sunahara, M., Shishikura, T., Nakamura, Y., Sakiyama, S., Seki, N., Ohira, M., Kaneko, Y., McKeon, F., Caput, D., and Nakagawara, A. (2001) *Med. Pediatr. Oncol.* **36,** 42–44
39. Bagchi, A., Papazoglu, C., Wu, Y., Capurso, D., Brodt, M., Francis, D., Bredel, M., Vogel, H., and Mills, A. A. (2007) *Cell* **128,** 459–475
40. Sells, S. F., Han, S. S., Muthukkumar, S., Maddiwar, N., Johnstone, R., Boghaert, E., Gillis, D., Liu, G., Nair, P., Monnig, S., Collini, P., Mattson, M. P., Sukhatme, V. P., Zimmer, S. G., Wood, D. P., Jr., McRoberts, J. W., Shi, Y., and Rangnekar, V. M. (1997) *Mol. Cell. Biol.* **17,** 3823–3832
41. Dutta, K., Engler, F. A., Cotton, L., Alexandrov, A., Bedi, G. S., Colquhoun, J., and Pascal, S. M. (2003) *Protein Sci.* **12,** 257–265
42. Joshi, B., Ko, D., Ordonez-Ercan, D., and Chellappan, D. (2003) *Biochem. Biophys. Res. Commun.* **312,** 459–466
43. Bharadwaj, R., and Yu, H. (2004) *Oncogene* **23,** 2016–2027
44. Endow, S. A. (1999) *Eur. J. Biochem.* **262,** 12–18
45. Nakagawara, A. (1998) *Med. Pediatr. Oncol.* **31,** 113–115
46. Nakagawara, A., Arima-Nakagawara, M., Scavarda, N. J., Azar, C. G., Cantor, A. B., and Brodeur, G. M. (1993) *N. Engl. J. Med.* **328,** 847–854
47. Midorikawa, R., Takei, Y., and Hirokawa, N. (2006) *Cell* **125,** 371–383

LETTERS

Oncogenic mutations of ALK kinase in neuroblastoma

Yuyan Chen[1,2,3]*, Junko Takita[1,2,3]*, Young Lim Choi[4]*, Motohiro Kato[1,3], Miki Ohira[5], Masashi Sanada[2,3,6], Lili Wang[2,3,6], Manabu Soda[4], Akira Kikuchi[7], Takashi Igarashi[1], Akira Nakagawara[5], Yasuhide Hayashi[8], Hiroyuki Mano[4,6] & Seishi Ogawa[2,3,6]

Neuroblastoma in advanced stages is one of the most intractable paediatric cancers, even with recent therapeutic advances[1]. Neuroblastoma harbours a variety of genetic changes, including a high frequency of *MYCN* amplification, loss of heterozygosity at 1p36 and 11q, and gain of genetic material from 17q, all of which have been implicated in the pathogenesis of neuroblastoma[2–5]. However, the scarcity of reliable molecular targets has hampered the development of effective therapeutic agents targeting neuroblastoma. Here we show that the anaplastic lymphoma kinase (ALK), originally identified as a fusion kinase in a subtype of non-Hodgkin's lymphoma (NPM–ALK)[6–8] and more recently in adenocarcinoma of lung (EML4–ALK)[9,10], is also a frequent target of genetic alteration in advanced neuroblastoma. According to our genome-wide scans of genetic lesions in 215 primary neuroblastoma samples using high-density single-nucleotide polymorphism genotyping microarrays[11–14], the *ALK* locus, centromeric to the *MYCN* locus, was identified as a recurrent target of copy number gain and gene amplification. Furthermore, DNA sequencing of *ALK* revealed eight novel missense mutations in 13 out of 215 (6.1%) fresh tumours and 8 out of 24 (33%) neuroblastoma-derived cell lines. All but one mutation in the primary samples (12 out of 13) were found in stages 3–4 of the disease and were harboured in the kinase domain. The mutated kinases were autophosphorylated and displayed increased kinase activity compared with the wild-type kinase. They were able to transform NIH3T3 fibroblasts as shown by their colony formation ability in soft agar and their capacity to form tumours in nude mice. Furthermore, we demonstrate that downregulation of *ALK* through RNA interference suppresses proliferation of neuroblastoma cells harbouring mutated *ALK*. We anticipate that our findings will provide new insights into the pathogenesis of advanced neuroblastoma and that *ALK*-specific kinase inhibitors might improve its clinical outcome.

To identify oncogenic lesions in neuroblastoma, we performed a genome-wide analysis of primary tumour samples obtained from 215 neuroblastoma patients using high-density single-nucleotide polymorphism (SNP) arrays (Affymetrix GeneChip 250K *Nsp*I) (Supplementary Table 1). Twenty-four neuroblastoma-derived cell lines were also analysed (Supplementary Table 2). Interrogating over 250,000 SNP sites, this platform permits the identification of copy number changes at an average resolution of less than 12 kilobases (kb)[13,14].

Analysis of this large number of samples, consisting of varying disease stages, permitted us to obtain a comprehensive registry of genomic lesions in neuroblastoma (Supplementary Figs 1 and 2). A gain of chromosomes, often triploid or hyperploid (defined by mean copy number of >2.5), was a predominant feature of neuroblastoma genomes in the lower stages. Ploidy generally correlated with the clinical stage, where non-hyperploid cases were significantly associated with stage 4 disease ($P = 4.13 \times 10^{-5}$, trend test) (Supplementary Fig. 3 and Supplementary Table 3). 17q gains, frequently in multiple copies ($3 \leq$ copy number < 5), were a hallmark of the neuroblastoma genome[4] and were found in most neuroblastoma cases. Copy number gains tended to spare chromosomes 3, 4, 10, 14 and 19 (Supplementary Figs 2 and 3). Notably, these chromosomes often had copy number losses including 1p (22.8%), 3p (8.8%), 4p (5.1%), 6q (7.0%), 10q (9.8%), 11q (19.5%), 14q (3.7%), 19p (7.4%) and 19q (5.1%), implicating the pathogenic role of 'relative' gene dosages.

After excluding known copy number variations, we identified a total of 28 loci undergoing high-grade amplifications (copy number ≥5) (Supplementary Table 4). These lesions fell into relatively small genomic segments, having a mean size of 361 kb, which accelerated the identification of gene targets in these regions (Supplementary Table 4 and Supplementary Fig. 4). The candidate gene targets included *TERT* (5p15.33), *HDAC3* (5q31.3), *IGF2* (11p15.1), *MYEOV* (11q13.3), *FGF7* (15q21.1) and *CDH13* (16q23.3). However, many of them were not recurrent but found only in a single case. Although the recurrent lesions were mostly explained by the amplification of *MYCN* at 2p24, as found in 50 out of 215 (23%) of the primary cases, we identified another peak of recurrent amplification at 2p23 (Fig. 1a), which consisted of amplicons in five primary cases and in one neuroblastoma-derived cell line, NB-1 (Supplementary Fig. 5). This peak was located at the centromeric margin of the common copy number gains in chromosome 2p, which was created by copy number gains in 109 samples mostly from non-hyperploid stage 4 cases. The minimum overlapping amplification was defined by the amplicons found in the NB-1 cell line (Supplementary Fig. 5) and contained a single gene, the anaplastic lymphoma kinase (*ALK*), which has previously been reported to be overexpressed in neuroblastoma cases[15]. Although five of the six samples showing *ALK* amplification also had *MYCN* amplification, one primary case (NT056) lacked a *MYCN* peak and the amplification was confined to the *ALK*-containing locus. In interphase fluorescent *in situ* hybridization (FISH) analysis of NB-1, *MYCN* and *ALK* loci were amplified in separate amplicons (Fig. 1b), indicating that the 2p23 amplicons containing *ALK* were unlikely to represent merely 'passenger' events of *MYCN* amplification but actively contributed to the pathogenesis of neuroblastoma.

Because an oncogene can be activated by gene amplification and/or mutation, to search for possible mutations we performed DNA heteroduplex formation analysis[16] and genomic DNA sequencing for the exons 20 to 28 of *ALK*, which encompass the juxtamembrane and kinase domains (Supplementary Table 5). In total, we identified eight nucleotide changes in 21 neuroblastoma samples, 13 out of 215

[1]Department of Pediatrics, [2]Cell Therapy and Transplantation Medicine, [3]Cancer Genomics Project, Graduate School of Medicine, The University of Tokyo, Tokyo 113-8655, Japan. [4]Division of Functional Genomics, Jichi Medical University, Toguchi 329-0498, Japan. [5]Division of Biochemistry, Chiba Cancer Center Research Institute, Chiba 260-8717, Japan. [6]Core Research for Evolutional Science and Technology, Japan Science and Technology Agency, Saitama, 332-0012, Japan. [7]Division of Hematology/Oncology, Saitama Children's Medical Center, Saitama 339-8551, Japan. [8]Gunma Children's Medical Center, Shibukawa 377-8577, Japan.
*These authors contributed equally to this work.

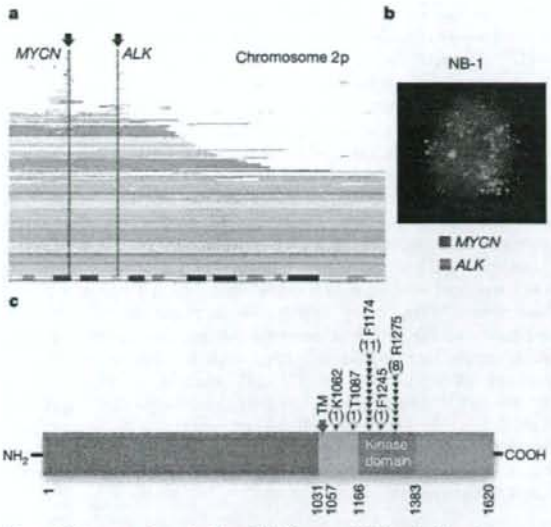

Figure 1 | Common 2p gains/amplifications and *ALK* mutations in neuroblastoma samples. a, Recurrent copy number gains on the 2p arm. High-grade amplifications are shown by light-red horizontal lines, whereas simple gains are shown by dark-red lines. Two common peaks of copy number gains and amplifications in the *MYCN* and *ALK* loci are indicated by arrows. The cytobands in 2p are shown at the bottom. **b**, Interphase FISH analysis of NB-1 showing high-grade amplification of *MYCN* (red) and *ALK* loci (green). The amplified *MYCN* locus appears as a single large signal. **c**, Distribution of the eight *ALK* mutations found in 21 neuroblastoma samples. The positions of the mutated amino acids are indicated by black (primary samples) and red (cell lines) arrowheads. The number of mutations at each site is shown at the top of the arrowheads. TM, transmembrane.

(6.1%) primary samples and 8 out of 24 (33%) cell lines, which resulted in seven types of amino acid substitutions at five different positions (Table 1 and Supplementary Fig. 6). They were not found in either the genomic DNA collected from 50 healthy volunteers or in the SNP databases at the time of preparing this manuscript. In fact, somatic origins of missense changes were confirmed in 9 out of 13 primary cases, for which DNA was obtained from the peripheral blood or the tumour-free bone marrow specimens (Supplementary Fig. 6). On the other hand, T1087I (ACC>ATC), found in case NT126, had a germline origin and thus it could not be determined whether the T1087I change was a rare non-functional polymorphism or represented a pathogenic germline mutation. For other changes found in three primary cases (NT128, NT217 and NT218) and cell lines, normal DNA was not available but they were likely to represent oncogenic mutations because they were identical to common somatic changes (F1174L or R1275Q) or shown to have oncogenic potential in functional assays (K1062M).

Most mutations occurred within the kinase domain (20 out of 22 or 91%), which clearly showed two mutation hotspots at F1174 and R1275 (Fig. 1c). A neuroblastoma-derived cell line, SJNB-2, had a homozygous *ALK* mutation of R1275Q, which was probably due to uniparental disomy of chromosome 2 (Supplementary Fig. 7a). Another case (NT074) harboured two different mutations, F1174L and R1275Q, but it remains to be determined whether both are on the same allele. ALK mutations within the kinase domain occurred at amino acid positions that are highly conserved across species and during molecular evolution (Supplementary Figs 8 and 9). According to the conserved structure of other insulin receptor kinases we predicted that F1174 is located at the end of the Cα1 helix, whereas the other two are on the two β-sheets: before the catalytic loop (β6, F1245) and within the activation loop (β9, R1275) (Supplementary Fig. 7b, c)[17]. Thus, conformational changes due to amino acid substitutions at these positions might be responsible for the aberrant activity of the mutant kinases.

Table 1 | *ALK* mutations/amplifications in neuroblastoma samples

Sample	Age (months)	Stage	*MYCN**	Clinical outcome	Mutations/ amplifications	Nucleotide substitution	Origin of mutations
NT126	99	4	−	Dead	T1087I	ACC>ATC	Germ line
NT218	8	1	−	Alive	F1174L	TTC>TTG	ND
NT074	34	3	+	Dead	F1174L	TTC>TTA	Somatic
					R1275Q	CGA>CAA	
NT160	12	4	+	Dead	F1174L	TTC>TTA	Somatic
NT217	24	4	+	Dead	F1174L	TTC>TTA	ND
NT190	48	4	+	Alive	F1174L	TTC>TTA	Somatic
NT060	163	3	−	Alive	F1174C	TTC>TGC	Somatic
NT162	28	4	+	Dead	F1174V	TTC>GTC	Somatic
NT195	24	4	+	Alive	F1245L	TTC>TTG	Somatic
NT055	6	3	−	Alive	R1275Q	CGA>CAA	Somatic
NT128	8	4	−	Dead	R1275Q	CGA>CAA	ND
NT164	54	4	+	Dead	R1275Q	CGA>CAA	Somatic
NT200	133	4	−	Dead	R1275Q	CGA>CAA	Somatic
SCMC-N5†	-	-	+	-	K1062M	AAG>ATG	ND
SJNB-4†	-	-	+	-	F1174L	TTC>TTA	ND
LAN-1†	-	-	+	-	F1174L	TTC>TTA	ND
SCMC-N2†	-	-	+	-	F1174L	TTC>TTA	ND
SK-N-SH†	-	-	−	-	F1174L	TTC>TTA	ND
SJNB-2†‡	-	-	+	-	R1275Q	CGA>CAA	ND
LAN-5†	-	-	+	-	R1275Q	CGA>CAA	ND
TGW†	-	-	+	-	R1275Q	CGA>CAA	ND
NT204	12	1	+	Alive	Amplification	-	-
NT056	11	3	−	Dead	Amplification	-	-
NT071	36	3	+	Alive	Amplification	-	-
NT165	19	4	+	Dead	Amplification	-	-
NT169	7	4	+	Dead	Amplification	-	-
NB-1†	-	-	+	-	Amplification	-	-

ND, not determined.
*Presence (+) or absence (−) of *MYCN* amplification in FISH analysis. All cases where there was an absence of *MYCN* amplification (−) were also checked for possible *MYCN* mutations by sequencing of all *MYCN* exons, but no *MYCN* mutations were identified.
†Cell lines.
‡Homozygous mutation.

ALK mutation highly correlated with *MYCN* amplification ($P = 1.55 \times 10^{-4}$, Fisher's exact test; Supplementary Table 6) where 14 out of 21 mutations coexisted with *MYCN* amplification. Regardless of the status of *MYCN* amplification, 12 of the 13 mutations were found in patients with advanced stage neuroblastoma (Table 1). However, whereas *MYCN* amplification and stage 4 were significant risk factors for poor survival, the mutation/amplification status of *ALK* was not likely to have a major impact on survival (Supplementary Fig. 10 and Supplementary Table 7), although the statistical power of the current analysis was largely limited in order to detect a marginal hazard.

To evaluate the impact of ALK mutations on kinase activity, we generated Flag-tagged constructs of ALK and its mutants, F1174L and K1062M, which were stably expressed in NIH3T3 cells, and examined their phosphorylation status and *in vitro* kinase activity. The ALK mutants stably expressed in NIH3T3 cells were phosphorylated according to western blot analysis using an antibody specific for phosphorylated ALK (anti-pY1604) and a PY20 blot after anti-Flag immunoprecipitation of the mutant kinases (Fig. 2a), whereas the wild-type kinase was not phosphorylated. The immunoprecipitated ALK mutants also showed increased tyrosine kinase activity *in vitro* when compared with wild-type ALK. This was shown using both a universal substrate for tyrosine kinase (poly-GluTyr) and the synthetic YFF peptide[18], which was derived from a sequence of the activation loop of *ALK* (Fig. 2b, c). In accordance with these findings, downstream molecules of ALK signalling including AKT, STAT3 and ERK[15] were activated in cells expressing mutant ALK, as shown by their increased phosphorylation (Fig. 2d).

Next, we investigated the oncogenic potential of these mutants. NIH3T3 cells stably expressing mutant kinases showed increased colony formation in soft agar compared with the wild-type protein (Fig. 3a and Supplementary Fig. 11). The tumorigenicity of these ALK mutants was further assayed by injecting 1.0×10^7 NIH3T3 cells into nude mice. The NIH3T3 cells transfected with the ALK mutants showed focus-forming capacity and developed subcutaneous tumours (6 out of 6 inoculations) 21 days after inoculation, whereas the mock and wild-type ALK-transfected cells did not (0 out of 6 inoculations) (Fig. 3b, c). Finally, we examined the effect of ALK inhibition on the proliferation of neuroblastoma-derived cell lines. RNA interference (RNAi)-mediated *ALK* knockdown resulted in reduced cell proliferation of SK-N-SH cells harbouring the F1174L mutation, but the effects were less clear in wild-type ALK-expressing LAN-2 cells (Fig. 3d, e). Of particular interest is a recent report that 5 out of 17 neuroblastoma-derived cell lines, including SK-N-SH and NB-1, frequently showed high sensitivity to the specific ALK inhibitor TAE684 (ref. 19).

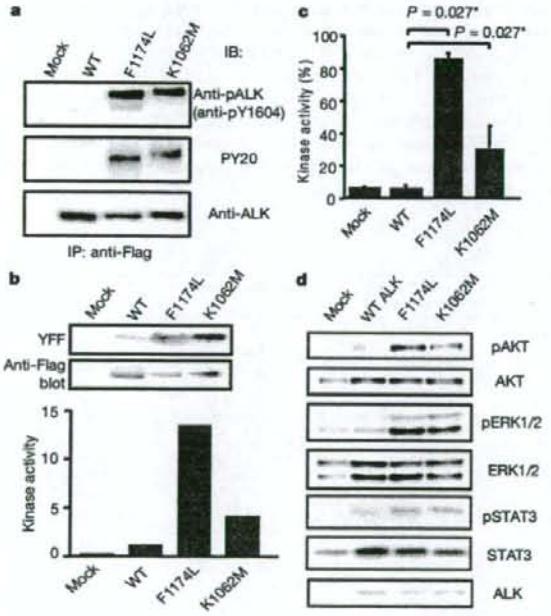

Figure 2 | Kinase activity of ALK mutants and their downstream signalling. **a**, Stably expressed ALK and its mutants (F1174L and K1062M) were immunoprecipitated with an anti-Flag antibody and subjected to western blot analysis with anti-pY1604 (upper panel) or PY20 (middle panel). An anti-ALK blot of precipitated kinases is also displayed (bottom panel). **b**, *In vitro* kinase assay for wild-type ALK kinase and its mutants using the synthetic YFF peptide as a substrate, where kinase activity is expressed as relative values to that for wild-type kinase based on the densities in the autoradiogram. **c**, Kinase activity was also assayed for the poly-GluTyr peptide. Significantly different measurements are indicated by asterisks with *P* values. Bars show mean (±s.d.) in three independent experiments. **d**, Western blot analyses of NIH3T3 cells expressing wild-type and mutant ALK for phosphorylated forms of AKT (pAKT), ERK (pERK1/2) and STAT3 (pSTAT3). The total amount of each molecule is also displayed (AKT, ERK1/2, and STAT3) together with an anti-ALK blot (ALK).

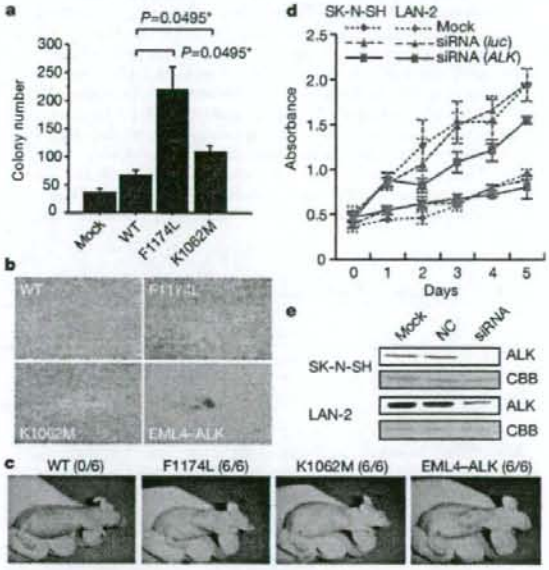

Figure 3 | Oncogenic role of ALK mutations. **a**, Colony assays for NIH3T3 cells stably expressing wild-type as well as mutant ALK (F1174L and K1062M). The average numbers of colonies in triplicate experiments are plotted and standard deviation is indicated. Results showing statistically significant differences as compared with experiments using wild-type ALK are indicated by asterisks with *P* values. **b**, **c**, NIH3T3 cells were transfected with wild-type and mutant ALK (F1174L, K1062M and EML4–ALK) and subjected to a focus forming assay (**b**) as well as an *in vivo* tumorigenicity assay in nude mice (**c**). **d**, Effect of RNAi-mediated ALK knockdown on cell proliferation in neuroblastoma cell lines expressing either the F1174L mutant (SK-N-SH) or wild-type ALK (LAN-2). Cell growth was measured using the Cell Counting Kit-8 after knockdown experiments using *ALK*-specific siRNAs (siRNA *ALK*), control siRNAs (siRNA *luc*), or mock experiments, where absorbance was measured in triplicate and averaged for each assay. To draw growth curves, the mean ± s.d. of the averaged absorbance in three independent knockdown experiments is plotted. **e**, Successful knockdown of ALK protein was confirmed by anti-ALK blots (ALK) using Coomassie brilliant blue G-250 (CBB) staining as loading controls. NC, control siRNA; siRNA, *ALK* siRNA.

Through the genome-wide analysis of genetic lesions in neuroblastoma, we identified novel oncogenic *ALK* mutations in advanced neuroblastoma. Combined with the cases having a high-grade amplification of the *ALK* gene, aberrant ALK signalling was likely to be involved in 11% (16 out of 151) of the advanced neuroblastoma cases. Because ALK kinase has been shown to be deregulated only in the form of a fusion kinase in human cancers, including lymphoma and lung cancer, the identification of oncogenic mutations in *ALK* not only increases our understanding of the molecular pathogenesis of advanced neuroblastoma, but also adds a new paradigm to the concept of 'ALK-positive human cancers' in that the mutated *ALK* kinases themselves might participate in human cancers. Our results again highlight the power of genome-wide studies to clarify the genetic lesions in human cancers[20–22]. Given that *ALK* mutations are preferentially involved in advanced neuroblastoma cases having a poor prognosis, our findings implicate that *ALK* inhibitors may improve the clinical outcome of children suffering from intractable neuroblastoma.

METHODS SUMMARY

Genomic DNA from 215 patients with primary neuroblastoma and 24 neuroblastoma-derived cell lines was analysed on GeneChip SNP genotyping microarrays (Affymetrix GeneChip 250K *Nsp*I). After appropriate normalization of mean array intensities, signal ratios were calculated between tumours and anonymous normal references in an allele-specific manner, and allele-specific copy numbers were inferred from the observed signal ratios based on the hidden Markov model using CNAG/AsCNAR software[13,14]. *ALK* mutations were examined by DNA heteroduplex analysis and/or genomic DNA sequencing[16]. Full-length cDNAs for mutant *ALK* were isolated by high-fidelity PCR and inserted into pcDNA3 and pMXS. The expression plasmids were transfected into NIH3T3 cells using Effectene Transfection Reagent (Qiagen) or by calcium phosphate methods[9]. Western blot analysis of mutant ALK kinases, *in vitro* kinase assays, and tumour formation assays in nude mice were performed as previously described[9]. This study was approved by the ethics boards of the University of Tokyo and of the Chiba Cancer Center Research Institute.

Full Methods and any associated references are available in the online version of the paper at www.nature.com/nature.

Received 3 June; accepted 28 August 2008.

1. Maris, J. M., Hogarty, M. D., Bagatell, R. & Cohn, S. L. Neuroblastoma. *Lancet* **369**, 2106–2120 (2007).
2. Maris, J. M. *et al.* Loss of heterozygosity at 1p36 independently predicts for disease progression but not decreased overall survival probability in neuroblastoma patients: a Children's Cancer Group study. *J. Clin. Oncol.* **18**, 1888–1899 (2000).
3. Attiyeh, E. F. *et al.* Chromosome 1p and 11q deletions and outcome in neuroblastoma. *N. Engl. J. Med.* **353**, 2243–2253 (2005).
4. Bown, N. *et al.* Gain of chromosome arm 17q and adverse outcome in patients with neuroblastoma. *N. Engl. J. Med.* **340**, 1954–1961 (1999).
5. Brodeur, G. M., Seeger, R. C., Schwab, M., Varmus, H. E. & Bishop, J. M. Amplification of N-myc in untreated human neuroblastomas correlates with advanced disease stage. *Science* **224**, 1121–1124 (1984).
6. Shiota, M. *et al.* Anaplastic large cell lymphomas expressing the novel chimeric protein p80NPM/ALK: a distinct clinicopathologic entity. *Blood* **86**, 1954–1960 (1995).
7. Morris, S. W. *et al.* Fusion of a kinase gene, ALK, to a nucleolar protein gene, NPM, in non-Hodgkin's lymphoma. *Science* **263**, 1281–1284 (1994).
8. Fujimoto, J. *et al.* Characterization of the transforming activity of p80, a hyperphosphorylated protein in a Ki-1 lymphoma cell line with chromosomal translocation t(2;5). *Proc. Natl Acad. Sci. USA* **93**, 4181–4186 (1996).
9. Soda, M. *et al.* Identification of the transforming *EML4–ALK* fusion gene in non-small-cell lung cancer. *Nature* **448**, 561–566 (2007).
10. Rikova, K. *et al.* Global survey of phosphotyrosine signaling identifies oncogenic kinases in lung cancer. *Cell* **131**, 1190–1203 (2007).
11. Kennedy, G. C. *et al.* Large-scale genotyping of complex DNA. *Nature Biotechnol.* **21**, 1233–1237 (2003).
12. Matsuzaki, H. *et al.* Genotyping over 100,000 SNPs on a pair of oligonucleotide arrays. *Nature Methods* **1**, 109–111 (2004).
13. Nannya, Y. *et al.* A robust algorithm for copy number detection using high-density oligonucleotide single nucleotide polymorphism genotyping arrays. *Cancer Res.* **65**, 6071–6079 (2005).
14. Yamamoto, G. *et al.* Highly sensitive method for genomewide detection of allelic composition in nonpaired, primary tumor specimens by use of affymetrix single-nucleotide-polymorphism genotyping microarrays. *Am. J. Hum. Genet.* **81**, 114–126 (2007).
15. Osajima-Hakomori, Y. *et al.* Biological role of anaplastic lymphoma kinase in neuroblastoma. *Am. J. Pathol.* **167**, 213–222 (2005).
16. Donohoe, E. Denaturing high-performance liquid chromatography using the WAVE DNA fragment analysis system. *Methods Mol. Med.* **108**, 173–187 (2005).
17. Hu, J., Liu, J., Ghirlando, R., Saltiel, A. R. & Hubbard, S. R. Structural basis for recruitment of the adaptor protein APS to the activated insulin receptor. *Mol. Cell* **12**, 1379–1389 (2003).
18. Donella-Deana, A. *et al.* Unique substrate specificity of anaplastic lymphoma kinase (ALK): development of phosphoacceptor peptides for the assay of ALK activity. *Biochemistry* **44**, 8533–8542 (2005).
19. McDermott, U. *et al.* Genomic alterations of anaplastic lymphoma kinase may sensitize tumors to anaplastic lymphoma kinase inhibitors. *Cancer Res.* **68**, 3389–3395 (2008).
20. Garraway, L. A. *et al.* Integrative genomic analyses identify MITF as a lineage survival oncogene amplified in malignant melanoma. *Nature* **436**, 117–122 (2005).
21. Mullighan, C. G. *et al.* Genome-wide analysis of genetic alterations in acute lymphoblastic leukaemia. *Nature* **446**, 758–764 (2007).
22. Kawamata, N. *et al.* Molecular allelokaryotyping of pediatric acute lymphoblastic leukemias by high-resolution single nucleotide polymorphism oligonucleotide genomic microarray. *Blood* **111**, 776–784 (2008).

Supplementary Information is linked to the online version of the paper at www.nature.com/nature.

Acknowledgements We thank H. P. Koeffler for critically reading and editing the manuscript. We also thank M. Matsumura, Y. Ogino, S. Ichimura, S. Sohma, E. Matsui, Y. Yin, N. Hoshino and Y. Nakamura for their technical assistance. This work was supported by the Core Research for Evolutional Science and Technology, Japan Science and Technology Agency and by a Grant-in-Aid from the Ministry of Health, Labor and Welfare of Japan for the third-term Comprehensive 10-year Strategy for Cancer Control.

Author Contributions Y.C., Y.L.C. and J.T. contributed equally to this work. M.K. and M.Sa. performed microarray experiments and subsequent data analyses. Y.C. and J.T. performed mutation analysis of *ALK*. Y.C., Y.L.C., J.T., M.So., L.W. and H.M. conducted functional assays of mutant ALK. A.N., M.O., T.I., A.K. and Y.H. prepared tumour specimens and were involved in statistical analysis. A.N., Y.H., H.M., J.T. and S.O. designed the overall study, and S.O. and J.T. wrote the manuscript. All authors discussed the results and commented on the manuscript.

Author Information The nucleotide sequences of *ALK* mutations detected in this study have been deposited in GenBank under the accession numbers EU788003 (K1062M), EU788004 (T1087I), EU788005 (F1174L; TTC/TTA), EU788006 (F1174L; TTC/TTG), EU788007 (F1174C), EU788008 (F1174V), EU788009 (F1245L) and EU788010 (R1275Q). The copy number data as well as the raw microarray data will be accessible from http://www.ncbi.nlm.nih.gov/geo/ with the accession number GSE12494. Reprints and permissions information is available at www.nature.com/reprints. Correspondence and requests for materials should be addressed to S.O. (sogawa-tky@umin.net) or Y.H. (hayashiy-tky@umin.ac.jp).

METHODS

Specimens. Primary neuroblastoma specimens were obtained during surgery or biopsy from patients who were diagnosed with neuroblastoma and admitted to a number of hospitals in Japan. In total, 215 primary neuroblastoma specimens were subjected to SNP array analysis after informed consent was obtained from the parents of each patient. The patients were staged according to the International Neuroblastoma Staging System[23]. The clinicopathological findings are summarized in Supplementary Table 1. Twenty-four neuroblastoma-derived cell lines were also analysed by SNP array analysis (Supplementary Table 2). The SCMC-N2, SCMC-N4 and SCMC-N5 cell lines were established in our laboratory[24,25]. The SJNB series of cells and the UTP-N-1[26] cell line were gifts from A. T. Look and A. Inoue, respectively. The other cell lines used were obtained from the Japanese Cancer Resource Cell Bank (http://cellbank.nibio.go.jp/).

Microarray analysis. High molecular mass DNA was isolated from tumour specimens as well as from the peripheral blood or the bone marrow as described previously[24]. The DNA was subjected to SNP array analysis using Affymetrix GeneChip Mapping 50K and/or 250K arrays (Affymetrix) according to the manufacturer's suggested protocol. The scanned array images were processed with Gene Chip Operation software (GCOS)[13], followed by SNP calls using GTYE. Genome-wide copy number measurements and loss of heterozygosity detection were performed using CNAG/AsCNAR algorithms[14], which enabled an accurate determination of allele-specific copy numbers.

Confirmation of SNP array data. FISH and/or genomic PCR analysis confirmed the results of SNP array analyses as described previously[13]. PCR primer sets were designed to amplify several adjacent fragments inside and outside of the homozygously deleted regions in tumour samples.

Mutation analysis. Mutations in the *ALK* gene were examined in 239 neuroblastoma samples, including 24 cell lines, by denaturing high-performance liquid chromatography (DHPLC) using the WAVE system (Model 4500; Transgenomic) according to the manufacturer's suggested protocol[16]. The samples showing abnormal conformations were subjected to direct sequencing analysis using an ABI PRISM 3100 Genetic Analyser (Applied Biosystems). Using direct sequencing, mutation analysis of *MYCN* was also performed in seven cases with *ALK* alterations but not *MYCN* amplification. The primer sets used in this study are listed in Supplementary Table 5.

Transforming potential of *ALK* mutants. Total RNA was extracted from SJNB-1 (wild type), SCMC-N2 (F1174L) and SCMC-N5 (K1062M) cells as described previously[26]. First-strand cDNA was synthesized from RNA using Transcriptor Reverse Transcriptase and an oligo (dT) primer (Roche Applied Science). The resulting cDNA was then amplified by PCR using the KOD-Plus-Ver.2 DNA polymerase (Toyobo) and the primers sense 5′-TCAGAAGCTTTACCAAGGACTGTTCAGAGC-3′ and antisense 5′-AATTGCGGCCGCTACTTGTCATCGTCGTCCTTGTAGTCGGGCCCAGGCTG GTTCATGC-3′, thereby introducing a HindIII site at the 5′ terminus and a NotI site and a Flag sequence at the 3′ terminus. The HindIII–NotI fragments of *ALK* cDNA were subcloned into pcDNA3 to generate expression plasmids. After resequencing to confirm that they had no other mutations, the *ALK* plasmids were used for transfection into NIH3T3 cells using Effectene Transfection Reagent (Qiagen) according to the suggested manufacturer's protocol. The transfected NIH3T3 cells were selected in 800 μg ml^{-1} G418 for 2 weeks to obtain stably expressing clones.

To evaluate the phosphorylation status of ALK mutants, the cell lysates of stable clones were immunoprecipitated with antibodies to Flag (Sigma) and the resulting precipitates were subjected to western blot analysis with the antibody specific to pTyr 1604 (Cell Signaling Technology) of ALK and the generic anti-phosphotyrosine antibody (PY20). The *in vitro* kinase activity of ALK mutants was measured using a non-radioactive isotope solid-phase enzyme-linked immunosorbent assay using the Universal Tyrosine Kinase Assay kit (Takara) according to the manufacturer's suggested protocol. We also performed the *in vitro* kinase assay with the synthetic YFF peptide (Operon Biotechnologies) as described previously[28]. For anchorage-independent growth analysis, 1×10^3 stably transfected NIH3T3 cells were mixed in 0.3% agarose with 10% FBS-DMEM and plated on 0.6% agarose-coated 35-mm dishes. After culture for 28 days, the colonies of >0.1 mm in diameter were counted. The quantification of the colonies was from three independent experiments. To investigate the downstream signalling of ALK, western blot analysis was performed using the anti-ERK1/2, anti-phospho-ERK1/2, anti-AKT, anti-phospho-AKT, anti-STAT3 and anti-phospho-STAT3 antibodies (Cell Signaling Technology)[15].

The cDNA mutant of *ALK* was also inserted into the pMXS plasmid and the constructs were introduced into NIH3T3 cells by the calcium phosphate method as described previously[9]. The cells were then either cultured for 21 days or injected subcutaneously at six sites in three nude mice.

Inhibition of ALK through RNAi-mediated knockdown. To suppress the expression of the ALK protein, two different pairs of *ALK* siRNAs (*ALK* siRNA1 and *ALK* siRNA2) were obtained (Qiagen)[15]. The sequences were 5′-GAGUCUGGCAGUUGACUUCdTdT-3′ for *ALK* siRNA1 and 5′-GCUCCGGCGUGCCAAGCAGdTdT-3′ for *ALK* siRNA2. A siRNA, targeting a sequence in firefly (*Photinus pyralis*) luciferase mRNA (*luc* siRNA), was used as a negative control (Qiagen)[15]. The sequences of *luc* siRNA were as follow: sense 5′-CGUACGCGGAAUACUUCGAdTdT-3′ and antisense 5′-UCGAAGUAUUCCGCGUACGdTdT-3′. Gene knockdown was achieved in SK-N-SH and LAN-2 cells using HiPerFect transfection reagent following the manufacturer's suggested instructions (Qiagen). To assess the effect of ALK knockdown on cell growth, these cells were seeded in 96-well plates at a concentration of 8.0×10^3 cells per well 24 h before transfection and assayed using the Cell Counting Kit-8 (Wako).

Statistical analysis. The significance of the correlation between *MYCN* amplification and *ALK* mutation was tested according to the conventional 2×2 contingency table using Fisher's exact test. The significance of the differences in kinase activity between wild-type and mutant ALK kinases was examined by the Mann–Whitney *U*-test based on the measured percentage activity of kinases in the precipitates of the corresponding samples. The significance of the differences in colony formation between wild-type and mutant ALK kinases was also examined by the Mann–Whitney *U*-test. The size of the hazards from possible risk factors, including International Neuroblastoma Staging System stages, *MYCN* status and *ALK* mutation/amplification were estimated by Cox regression analysis assuming a proportional hazard model using Stata software. Correlation between ploidy and clinical stage was tested by nptrend test.

23. Smith, E. I., Haase, G. M., Seeger, R. C. & Brodeur, G. M. A surgical perspective on the current staging in neuroblastoma—the International Neuroblastoma Staging System proposal. *J. Pediatr. Surg.* **24**, 386–390 (1989).
24. Takita, J. *et al.* Allelotype of neuroblastoma. *Oncogene* **11**, 1829–1834 (1995).
25. Takita, J. *et al.* Absent or reduced expression of the caspase 8 gene occurs frequently in neuroblastoma, but not commonly in Ewing sarcoma or rhabdomyosarcoma. *Med. Pediatr. Oncol.* **35**, 541–543 (2000).
26. Takita, J. *et al.* Allelic imbalance on chromosome 2q and alterations of the caspase 8 gene in neuroblastoma. *Oncogene* **20**, 4424–4432 (2001).

Plasma midkine level is a prognostic factor for human neuroblastoma

Shinya Ikematsu,[1] Akira Nakagawara,[2] Yohko Nakamura,[2] Miki Ohira,[2] Masaki Shinjo,[3] Satoshi Kishida[4] and Kenji Kadomatsu[4,5]

[1]Department of Bioresources Engineering, Okinawa National College of Technology, Okinawa 905-2192; [2]Division of Biochemistry, Chiba Cancer Research Center Research Institute, Chiba 260-8717; [3]Department of Public Health and Epidemiology, Okinawa Prefectural College of Nursing, Okinawa 902-0076; [4]Department of Biochemistry, Nagoya University Graduate School of Medicine, Nagoya 466-8550, Japan

(Received December 23, 2007/Revised June 3, 2008/Accepted June 27, 2008/Online publication October 21, 2008)

Neuroblastoma is the third-most-common solid tumor of childhood. To date, no reliable blood marker for neuroblastoma has been established. The growth factor midkine is highly expressed in human carcinomas and its knockdown leads to tumor growth suppression in animal models. The present study evaluated the plasma midkine level in human neuroblastoma patients. Plasma samples were obtained from patients found through mass screening, as well as from sporadic neuroblastoma patients. The total number of cases examined was 756. Among them, prognostic information was available for 175 sporadic cases and 287 mass-screening cases. Midkine levels were significantly higher in neuroblastoma patients, including both mass-screening cases and sporadic cases, than in non-tumor controls ($P < 0.0001$). The midkine level was significantly correlated with the statuses of *MYCN* amplification, *TRKA* expression, ploidy, stage and age ($P < 0.0001$, < 0.0001, $= 0.004$, < 0.0001 and < 0.0001, respectively), which are known prognostic factors for neuroblastoma. There was a striking correlation between high plasma midkine level and poor prognosis ($P < 0.0001$). Within sporadic cases, the midkine level was also strikingly higher than in non-tumor controls ($P < 0.0001$), and correlated with the statuses of *MYCN* amplification and stage ($P = 0.0005$ and $= 0.003$, respectively). There was a significant correlation between high plasma midkine level and poor prognosis ($P = 0.04$). Taken together, the present data indicate that plasma midkine level is a prognostic factor for human neuroblastoma. (*Cancer Sci* 2008; 99: 2070–2074)

Neuroblastoma (NBL) is the third-most-common malignant tumor of childhood, accounting for 15% of cancer-related death.[1] In spite of an enormous amount of research devoted to curing this disease, its prognosis remains poor. NBL has several established prognostic factors, i.e. *MYCN* amplification, *TRKA* expression level, ploidy, stage and age.[1,2] Cases with tumors with an amplified *MYCN* gene, low *TRKA* expression or diploidy show poor prognosis. Cases at stage 3 or 4, or at ages older than 18 months also show poor prognosis. Since molecular fingerprints within tumor tissues, such as *MYCN* amplification, *TRKA* expression level and ploidy, require a tumor biopsy or its removal, a blood marker for NBL has long been awaited.[1,2] A blood marker would not only be useful for the initial diagnosis but would also be beneficial for the sequential monitoring of the tumor status.

The growth factor midkine (MK) was originally found in embryonal carcinoma cells, and has been implicated in cancer development.[3–5] MK is highly and frequently expressed in human carcinomas, including Wilms' tumor, tumors of the digestive tract, brain tumors, urinary bladder tumors and breast tumors, whereas its expression is scarcely detected in normal adult tissues.[6–10] Strong MK expression is also detected in precancerous stages of human colorectal cancer and human prostate cancer.[11,12] Knockdown of MK expression leads to suppression of xenografted tumors of mouse colorectal cancer cells and human prostate cancer cells.[13,14]

We previously reported that the plasma MK level was correlated with the values of established prognostic factors through a study of 220 cases, including 82 non-mass-screening (sporadic) cases and 122 mass-screening cases.[15] However, in that study, information on the prognosis of patients was too limited to determine whether the plasma MK level could be a prognostic factor. In the present study, we measured plasma MK levels of 756 NBL cases, which consisted of 286 sporadic cases, 387 mass-screening cases and 83 unknown cases. Among them, prognostic information was available for 175 sporadic cases and 287 mass-screening cases. This enabled us to evaluate the plasma MK level as a prognostic factor.

Mass screening for NBL started in 1985 in Japan, but was discontinued in 2004 because of the lack of apparent beneficial effects on the cure rate of NBL. Mass-screening cases are grouped into the favorable prognosis group, and most of the mass-screening cases are thought to have spontaneously regressed. Therefore, nowadays, sporadic NBL patients are the major subject of therapy. However, information obtained from mass-screening cases has been useful, especially to understand tumor phenotype with favorable prognosis. This is the reason why we enrolled 387 mass-screening patients in this study. Accordingly, we evaluated plasma MK levels in two categories: first, the entire set of NBL cases including mass-screening cases and sporadic cases; and second, the set of sporadic cases.

Here we report that the plasma MK level is a prognostic factor for NBL.

Materials and Methods

Plasma samples. Clinical data of 756 neuroblastoma patients are summarized in Table 1. The same archive samples were used as those without malignant tumors ($n = 17$; eleven were <1-year old and six were >1-year old).[15]

Enzyme-linked immunoassay for human MK. An enzyme-linked immunoassay for human MK was performed as described previously.[16] Briefly, human MK was produced using *Pichia pastoris* GS115 by transfection with a human MK expression vector, which was constructed into pHIL-D4 (Invitrogen, Carlsbad, CA, USA). This yeast-produced human MK was used to immunize rabbits and chickens to raise antibodies. The rabbit antihuman MK antibody (50 μL of 5.5 μg/mL in 50 mM Tris HCl (pH 8.2), 0.15 M NaCl, 0.1% NaN_3) was coated onto the wells of microtiter plates (Polysorp plates, Nunc, Rochester, New York, USA) for 20 h at room temperature. After washing with 0.05% Tween-20 in phosphate-buffered saline (PBS), the wells were

[5]To whom correspondence should be addressed.
E-mail: kkadoma@med.nagoya-u.ac.jp

doi: 10.1111/j.1349-7006.2008.00957.x